Electronic Supplementary Material (ESI) for Chemical Communications.

Electronic Supplementary Information

Turning on ROP activity in a bimetallic Co/Zn complex supported by a [2+2] Schiff-base macrocycle

Kuiyuan Wang, Timothy J. Prior and Carl Redshaw*

Department of Chemistry & Biochemistry, University of Hull, Hull, HU6 7RX, U.K.

Contents

ROP experimental

Figure S8. X-ray diffraction data collected from a polycrystalline sample of complex **1*Me***·4MeCN using Mo Kα radlated diffraction data from the structure determined by single crystal diffraction.

Figure S9. Calculated (black lines) and found powder X-Ray diffraction (PXRD) patterns of **1*t*Bu**·0.5MeCN.

Figure S10. ^{1}H NMR (400 MHz $CDCl_3$) spectrum for **3Me**·MeCN

Figure S11. ^{1}H NMR (400 MHz $CDCl_3$) spectrum for **3*t*Bu**·MeCN***.***

Figure S12. Calculated (black lines) and found powder X-Ray diffraction (PXRD) patterns of **3*t*Bu**·MeCN.

Figure S13. ^{1}H NMR (400 MHz $CDCl_3$) spectrum for **5Me**·3MeCN at 22 ^{o}C.

Figure S14. ^{1}H NMR (400 MHz $CDCl_3$) spectrum for **5Me**·3MeCN at 130 ^{o}C.

Figure S15. X-ray diffraction data collected from a polycrystalline sample of complex **5Me**·3MeCN using Mo Kα radiation and simulated diffraction data from the structure determined by single crystal diffraction.

Figure S16. ^{1}H NMR (400 MHz $CDCl_3$) spectrum for **5*t*Bu**·3.25MeCN at 22 ^{o}C.

Figure S17. ^{1}H NMR (400 MHz $CDCl_3$) spectrum for **5*t*Bu**·3.25MeCN at 130 ^{o}C.

Figure S18. X-ray diffraction data collected from a polycrystalline sample of complex **5*t*Bu**·3.25MeCN using Mo Kα radiation and simulated diffraction data from the structure determined by single crystal diffraction.

Figure S19. Relationship between conversion and time for the polymerization of δ-VL.

Figure S20. MALDI-ToF mass spectrum for polymer (δ-VL run 4).

Figure S21. Structure analysis of the polyvalerolactone.

Figure S22. ^{1}H NMR (400 MHz $CDCl_3$) spectrum for polymer (δ-VL run 4).

Figure S23. Gel permeation chromatography for δ-VL run 4.

Figure S24. Plot (log M_w) of polyvalerolactone formed for δ-VL run 4.

Figure S43. MALDI-ToF mass spectrum for Poly (ε-CL+*r*-LA). [Red: positive method in which we can see the gap of 114 which corresponding to the molecular weight of the ε-CL, Green: negative method in which we can see the gap of 144 which corresponding to the molecular weight of *r*-LA.]

ESI Material:

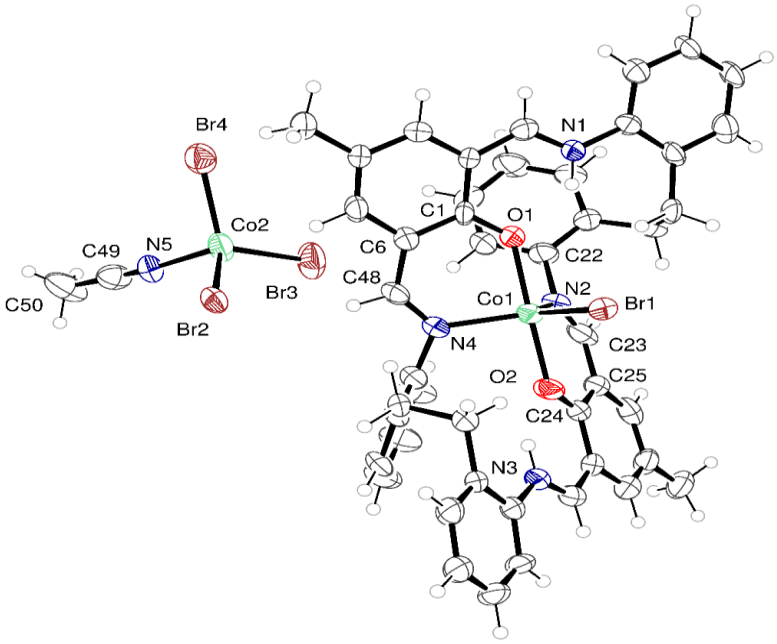

Figure S1. Molecular structure of minor orange product [CoBr**L**^{Me}][$CoBr_3$(NCMe)]·4MeCN (**1Me**·4MeCN). Solvent omitted for Clarity.

Selected bond lengths (Å) and angles (°): Co(1) – Br(1) 2.478(2), Co(1) – O(1) 2.025(8), Co(1) – O(2) 2.014(8), Co(1) – N(2) 2.048(11), Co(1) – N(4) 2.063(9); O(1) – Co(1) – O(2) 178.6(3), N(2) – Co(1) – N(4) 114.7(4), O(1) – Co(1) – Br(1) 88.9(2), N(2)-Co(1)-Br(1) 123.9(3)º, N(4)-Co(1)-Br(1) 121.4(3)º.

Crystal data for compound **1Me**·4MeCN*:* $C_{56}H_{55}Br_4Co_2N_9O_2$, *M* = 1323.59, monoclinic, space group C 2/c, *a* = 28.9470(7), *b* = 14.9123(3), *c* = 28.7611(8) Å, *α* = 90 *β* = 110.451(3), *γ* = 90 °, *V* = 11632.7(5) Å^3. *Z* = 8, *Dc* = 1.512 g cm^{-3}, F(000) = 5312, *T* = 100(2) K, μ(Mo-Kα) = 8.062 mm^{-1}, λ(Mo-Kα) = 1.54184 Å, θ_{max} = 68.25°, R_1 (*[I > 2σ(I)]* = 0.1081, wR_2 *(all data)* = 0.2946.

Crystal data for compound **1*t*Bu**·0.5MeCN: $C_{110}H_{110}Br_8Co_4N_{11}O_4$, *M* = 2525.08, triclinic, space group P-1, *a* = 10.7727(3), *b* = 12.2755(4), *c* = 21.8766(5) Å, *α* = 84.154(2) *β* = 88.514(2), *γ* = 65.975(3) °, *V* = 2628.22(14) $Å^3$. *Z* = 1, *Dc* = 1.593 g cm^{-3}, F(000) = 1263, *T* = 100(2) K, μ(Mo-Kα) = 3.718 mm^{-1}, λ(Mo-Kα) = 0.71075 Å, θ_{max} = 27.49°, R_1 (*[I > 2σ(I)]* = 0.046, wR_2 *(all data)* = 0.096. There is a pseudo two-fold symmetry axis along the Co-Br bond. In the macrocyclic ligand in **1*t*Bu**, there are four N atoms, each involved in a double bond, *viz* C11=N1 (1.288(4) Å), C26=N2 (1.313(4) Å), N3=C37 (1.289(4) Å), and N4=C52 1.310(5) Å). N1 and N3 are coordinated to the Co atom, while N2 and N4 are non-coordinating.

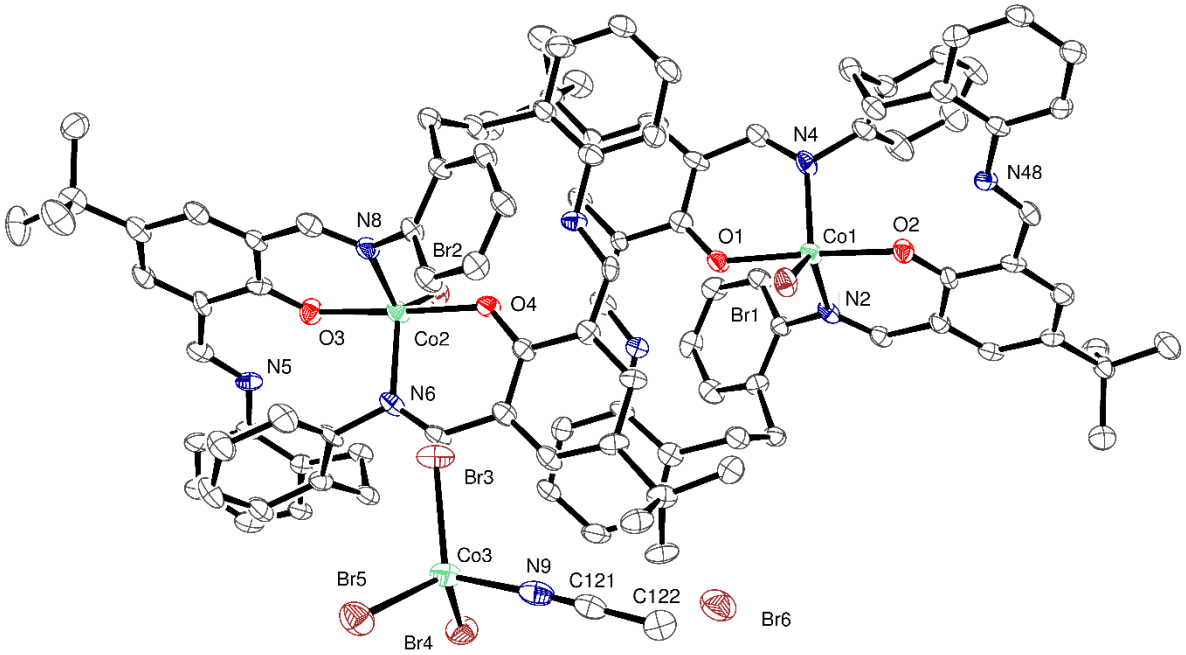

Figure S2. Molecular structure of minor orange product $[CoBrL^{tBu}]_2[CoBr_3(NCMe)][Br]$·4.5MeCN (**2*t*Bu**·4.5MeCN). Solvent omitted for Clarity.

Selected bond lengths (Å) and angles (°): Co(1)–Br(1) 2.4874(12), Co(1)–O(1) 2.041(4), Co(1)–O(2) 2.009(4), Co(1)–N(2) 2.072(6), Co(1)–N(4) 2.081(6); O(1)–Co(1)–O(2) 176.64(19), N(2)–Co(1) – N(4) 110.3(2), O(1)–Co(1)–Br(1) 86.10(15), Co(2)–Br(2) 2.4917(14), Co(2)–O(3) 2.009(6), Co(2)–O(4)

2.018(6), Co(2)–N(6) 2.085(7), Co(2)–N(8) 2.077(7); O(3)–Co(2)–O(4) 175.9(2), N(6)–Co(2)– N(8) 108.5(3), O(3)–Co(2)–Br(2) 88.77(18).

Crystal data for compound **2*t*Bu**·4.5MeCN*:* $C_{115}H_{117.5}Br_6Co_3N_{13.5}O_4$, *M* = 2408.97, triclinic, space group P 1, *a* = 14.2178(5), *b* = 15.0893(4), *c* = 15.4758(4) Å, *α* = 101.542(2), *β* = 113.361(3), *γ* = 106.394(3) °, *V* = 2734.40(16) $Å^3$. *Z* = 1, *Dc* = 1.460 g cm^{-3}, F(000) = 1221, *T* = 100(2) K, μ(Mo-Kα) = 2.7 mm^{-1}, λ(Mo-Kα) = 0.71075 Å, θ_{max} = 27.49°, R_1 *([I > 2σ(I)]* = 0.053, wR_2 *(all data)* = 0.129.

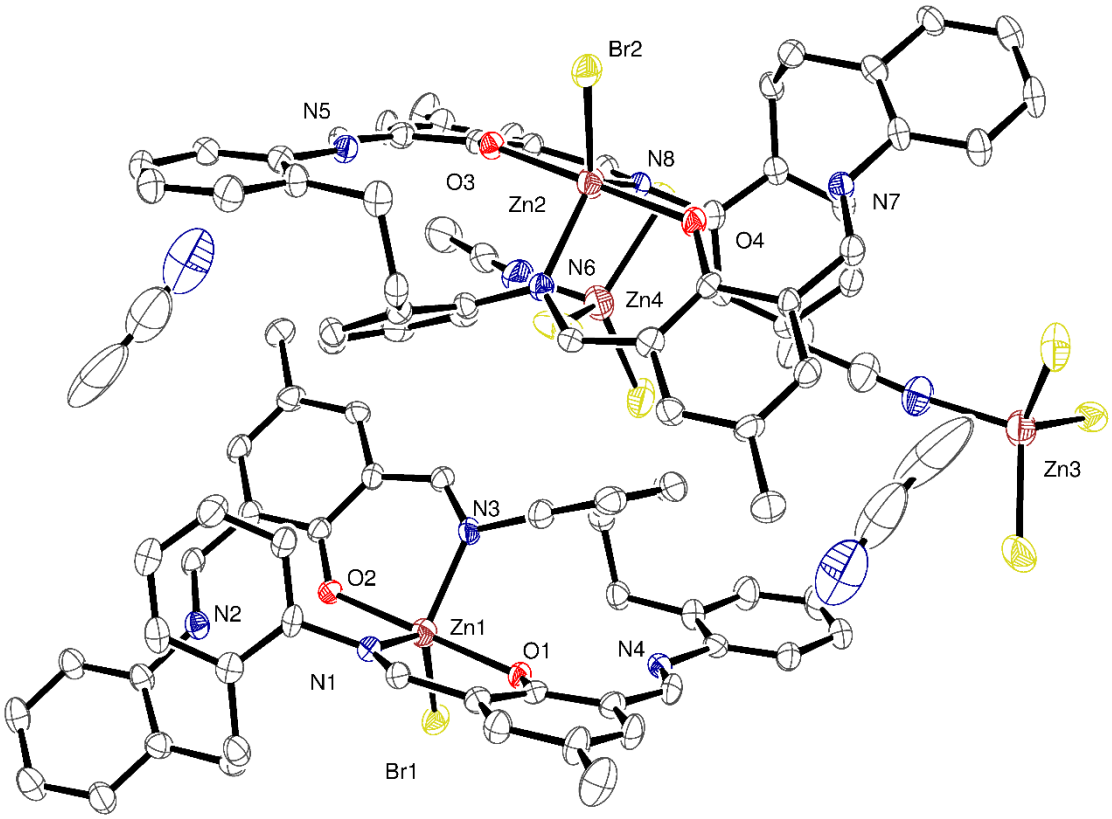

Figure S3. Molecular structure of [ZnBr$\mathbf{L^{Me}}$][$ZnBr_3$(NCMe)]·MeCN (**3Me**·MeCN). Thermal ellipsoids are drawn at the 30% probability level.

Selected bond lengths (Å) and angles (º): Zn(1)–Br(1) 2.4344(9), Zn(1)–O(1) 2.077(4), Zn(1)–O(2) 2.085(4), Zn(1)–N(1) 2.082(5), Zn(1)–N(3) 2.061(5); O(1)–Zn(1)–O(2) 179.74(18), N(1)–Zn(1)–N(3) 112.93(19), O(1)–Zn(1)–Br(1) 89.27(11), N(3)–Zn(1)–Br(1) 120.14(14), N(1)–Zn(1)–Br(1) 126.92(13)º.

Crystal data for compound **3Me**·MeCN*:* $C_{50}H_{46}Br_4N_6O_6Zn_2$, M_r = 1213.31, triclinic, space group P-1, a = 14.8222(4), b = 16.2435(4), c = 23.2841(5), α = 94.842(2), β = 93.195(2), γ = 115.593(3)°, V = 5011.3(2) Å^3, Z = 4, ρ_{calcd} = 1.605 Mg m^{-3}, λ*(Mo-Kα)* = 0.71075, T = 100(2) K, θ_{max} = 25.36°, R_1 *[I > 2σ(I)]* = 0.0602, wR_2 *(all data)* = 0.1837.

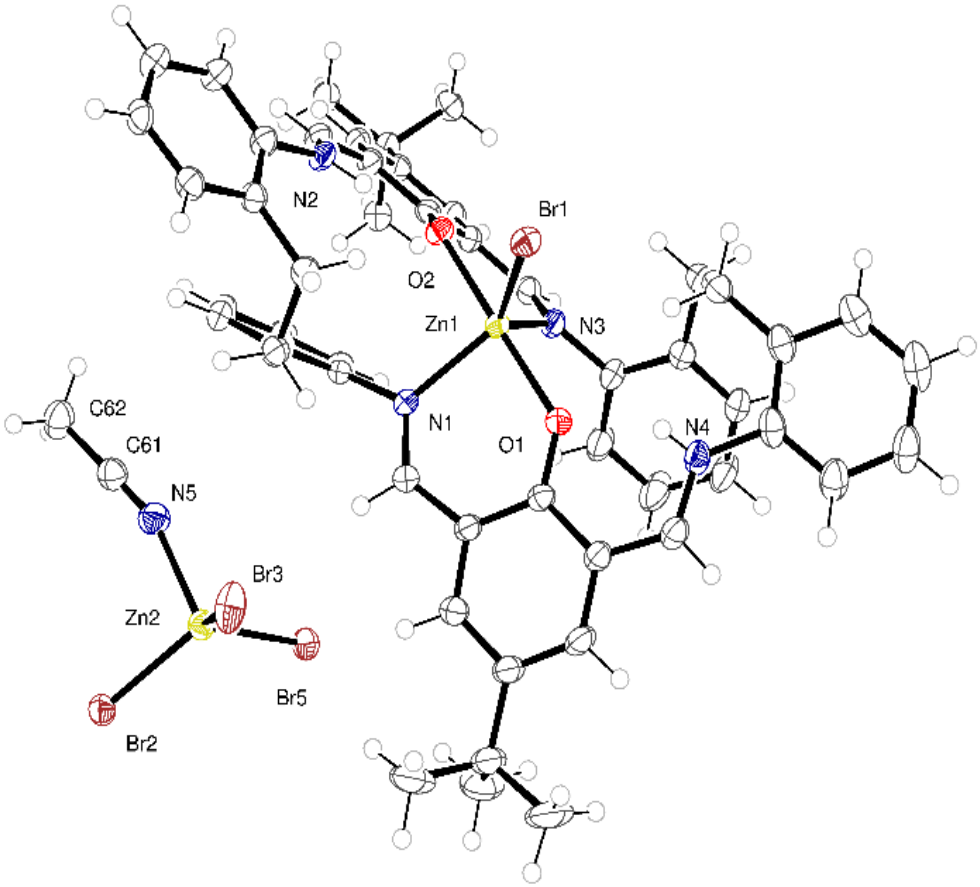

Figure S4. Molecular structure of [ZnBr**L**^{tBu}][$ZnBr_3$(NCMe)]·MeCN (**3*t*Bu**·MeCN). Solvent omitted for clarity. Solvent omitted for Clarity.

Thermal ellipsoids are drawn at the 30% probability level. Selected bond lengths (Å) and angles (°): Zn(1) – Br(1) 2.4502(4), Zn(1) – O(1) 2.0464(17), Zn(1) – O(2) 2.0383(16), Zn(1) – N(1) 2.107(2), Zn(1) – N(3) 2.117(2); O(1) – Zn(1) – O(2) 178.70(7), N(1) – Zn(1) – N(3) 110.37(8), O(1) – Zn(1) – Br(1) 92.86(5), N(3)-Zn(1)-Br(1), 126.86(6), N(1)-Zn(1)-Br(1) 122.65(6), N(1)-Zn(1)-N(3) 110.37(8).

Crystal data for compound **3*t*Bu**·MeCN: $C_{54.25}H_{55}Br_4N_5O_{2.25}Zn_2$, M_r = 1263.41, triclinic, space group P-1, a = 10.75900(10), b = 12.2903(2), c = 21.8932(3), α = 84.0830(10), β = 88.4630(10), γ = 66.072(2)°, V =

2631.71(7) Å^3, Z = 2, ρ_{calcd} = 1.594 Mg m^{-3}, λ*(Mo-Kα)* = 1.54184, T = 100(2) K, θ_{max} = 68.25°, R_1 *[I > 2σ(I)]* = 0.0298, wR_2 *(all data)* = 0.0799.

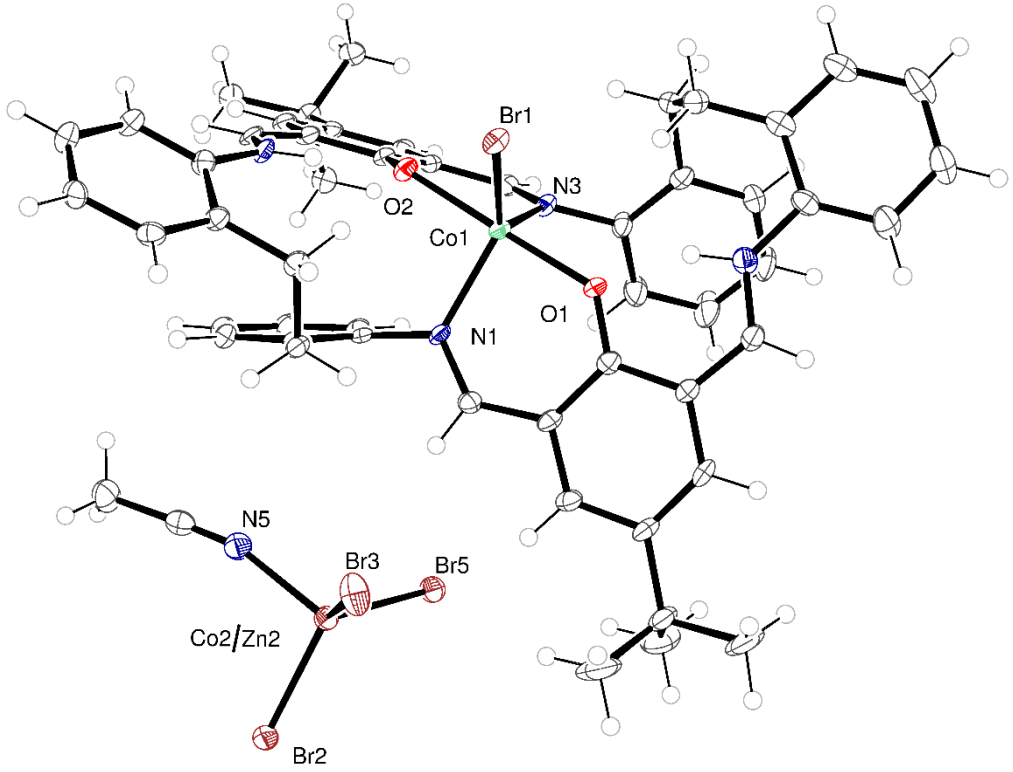

Figure S5. Molecular structure of [CoBr**L**^{tBu}][$Co_{0.68}Zn_{0.32}Br_3$(NCMe)]·0.25MeCN (**4*t*Bu**·0.25MeCN) Solvent omitted for clarity. Thermal ellipsoids are drawn at the 30% probability level. Selected bond lengths (Å) and angles (º): Co(1)–Br(1) 2.4847(6), Co(1)–O(11) 2.004(2), Co(1)–O(14) 2.043(2), Co(1)–N(37) 2.105(3), Co(1)–N(67) 2.088(3); O(11)–Co(1)–O(41) 178.52(9), N(37)–Co(1)–N(67) 108.77(11), O(11)–Co(1)–Br(1) 92.98(7), N(3)–Co(1)–Br(1) 127.99(8), N(1)–Co(1)–Br(1) 122.75(9), N(1)–Co(1)–N(3) 108.72(11)º.

Crystal data for compound **4*t*Bu**·0.25MeCN: $C_{54.50}H_{55}Br_4N_{5.25}O_2Co_{1.68}Zn_{0.32}$, M_r = 1255.07, triclinic, space group P -1, a = 10.7788(5), b = 12.2801(6), c = 21.8831(10) Å, α = 84.218(4), β = 88.620(4), γ = 66.052(4)°,

V = 2633.3(2) Å^3, Z = 2, ρ_{calcd} = 1.583 Mg m^{-3}, λ(*Mo-Kα*) = 0.71075, T = 100(2) K, θ_{max} = 26.37°, R_1 [$I > 2\sigma(I)$] = 0.034, wR_2 (*all data*) = 0.072.

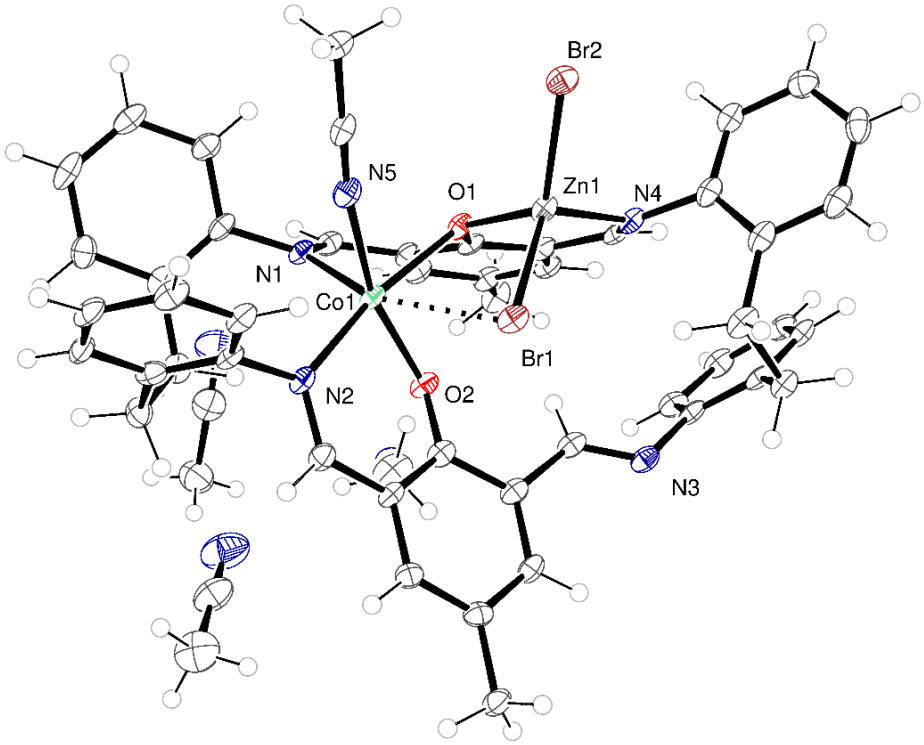

Figure S6. Molecular structure of [Co**L**^{Me} (NCMe)(μ-Br)ZnBr]·3MeCN (**5Me**·3MeCN).

Selected bond lengths (Å) and angles (º): Co(1) – O(1) 2.154(3), Co(1) – O(2) 1.960(3), Co(1) – N(1) 2.108(3), Co(1) – N(2) 2.071(3), Co(1) – N(5) 2.112(4), Co(1) – Br(1) 2.964(7), Zn(1) – O(1) 1.981(3), Zn(1) – Br(1) 2.3956(6), Zn(1) – Br(2) 2.3418(6), Zn(1) – N(4) 2.024(3); N(1) – Co(1) – N(2) 107.09(13), N(2) – Co(1) – O(2) 89.21(13), O(2) – Co(1) – N(5) 164.35(13), Co(1)-O(1)-Zn(1) 102.68(12)º, O(1)-Zn(1)-N(4) 93.72(13)º, Br(1)-Zn(1)-Br(2) 113.90(2)º.

Crystal data for compound **5Me**·3MeCN: $C_{48}H_{41}Br_2CoN_5O_2Zn$, M = 1127.14, monoclinic, space group P $2_1/c$, a = 14.6177(3), b = 17.0574(3), c = 21.1721(4) Å, α = 90, β = 108.948(2), γ = 90 °, V = 4993.00(17)

Å^3. Z = 4, Dc = 1.499 g cm^{-3}, F(000) = 2292, T = 100(2) K, μ(Mo-Kα) = 2.463 mm^{-1}, λ(Mo-Kα) = 0.71075 Å, θ_{max} = 25,03°, R_1 ($[I > 2\sigma(I)]$ = 0.056, wR_2 *(all data)* = 0.152.

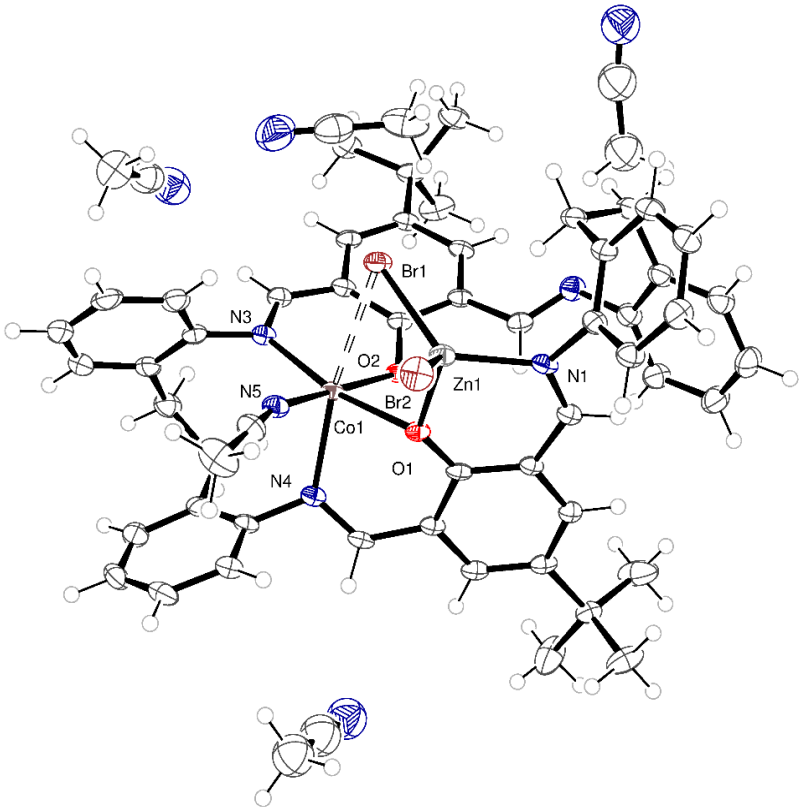

Figure S7. Alternative view of molecular structure of [Co**L**^{tBu}(NCMe)(μ-Br)ZnBr]·3¼MeCN (**5*t*Bu**·3.25MeCN).

Crystal data for compound **5*t*Bu**·3.25MeCN: $C_{242}H_{251}Br_8N_{33}O_8Co_4Zn_4$, M_r = 4886.22, monoclinic, space group P 2_1/c, a = 22.6868(2), b = 12.62670(10), c = 20.6141(2) Å, α = 90, β = 103.5260(10), γ = 90°, V = 5741.32(15) Å^3, Z = 1, ρ_{calcd} = 1.413 Mg m^{-3}, λ*(Mo-Kα)* = 0.71075, T = 100(2) K, θ_{max} = 27.48°, R_1 *[I > 2σ(I)]* = 0.047, wR_2 *(all data)* = 0.128.

Crystal Structure Determinations

Single crystal X-ray diffraction data were collected by the EPSRC UK National Crystallography Service for the majority of samples. Data collections were performed from crystals held at 100K, data for **1*t*Bu**·0.5MeCN were collected using a Mo rotating anode source and a Rigaku Oxford Diffraction 2015; Data for **1Me**·4MeCN and **3*t*Bu**·MeCN were collected using a Cu rotating anode source and a Rigaku HyPix 6000 detector; data for **2*t*Bu**·4.5MeCN and **3Me**·MeCN were collected using a Mo rotating anode source and a Rigaku HG Saturn724+ detector; data for **5Me**·3MeCN were collected using a Mo rotating anode source and a Rigaku HyPix 6000; data for **5*t*Bu**·3.25MeCN were collected using a Mo rotating anode source and a Rigaku Oxford Diffraction 2017;. Data were processed using Rigaku Oxford software. Single crystal X-ray diffraction data for **4*t*Bu**·0.25MeCN were collected using a Stoe IPDS2 image plate diffractometer operating with Mo radiation. The crystal was held at 150 K for the data collection. Raw data were processed using the Stoe X-AREA suite of programmes. Diffraction data were treated for the effects of absorption.

Structures were solved using dual-space methods within SHELXT [1] and refined against F^2 using all unique reflections with the program SHELXL-2018 [1] All non-hydrogen atoms were refined using anisotropic displacement parameters. Hydrogen atoms were placed using a riding model.

For **1Me**·4MeCN and **2*t*Bu**·4.5MeCN small scale disorder was modelled using standard techniques. **3Me**·MeCN is a non-merohedral twin (fractions 0.161(4): 0.839(4)); the refinement was conducted using data from both twin components. The structure is pseudo body centred. For reflections with h+k+l even, $\langle I/\sigma_I \rangle = 22.55$. For reflections with h+k+l odd, $\langle I/\sigma_I \rangle = 4.75$. These are systematically weak but not systematically absent. It is not possible to undertake a stable refinement in I-1.

Experimental procedures

General: All manipulations were carried out under an atmosphere of dry nitrogen using conventional Schlenk and cannula techniques or in a conventional nitrogen-filled glove box. Toluene was refluxed over sodium. Acetonitrile was refluxed over calcium hydride. THF was dried over sodium benzophenone. All solvents were distilled and degassed prior to use. IR spectra (nujol mulls, KBr windows) were recorded on a Nicolet Avatar 360 FT-IR spectrometer; ^{1}H NMR spectra were recorded at room temperature on a Varian VXR 400 S spectrometer at 400 MHz or a Gemini 300 NMR spectrometer or a Bruker Advance DPX-300 spectrometer at 300 MHz. The ^{1}H NMR spectra were calibrated against the residual protio impurity of the deuterated solvent. Magnetic moments were determined using an Evans balance. [2] Elemental analyses were performed by the elemental analysis service at the Department of Chemistry, the University of Hull. The pro-ligands **L**^{tBu}H$_2$ and **L**^{Me}H$_2$ were prepared as described previously. [3] All other chemicals were purchased from Sigma Aldrich or TCI, UK.

Synthesis of [CoBr**L**^{Me}][CoBr$_3$(NCMe)]·4MeCN (**1Me**·4MeCN)

L^{Me}H$_2$ (0.50 g, 0.73 mmol) and CoBr$_2$ (0.32 g, 1.47 mmol) were weighed out in a dry box. After transferring to a Schlenk line, toluene (20 mL) was added and the system was refluxed for 12 h. On cooling, the volatiles were removed *in-vacuo*, and the residue was extracted into warm MeCN (20 mL). On cooling (0 ^{o}C), green prisms were formed which were isolated and dried *in-vacuo* to afford **1Me**·4MeCN (0.66 g, 69% yield). Elemental analysis calculated for $C_{48}H_{41}Br_4Co_2N_5O_2$ (**1Me**): C 49.73, H 3.57, N 6.05%. Found: C 49.24, H 3.63, N 5.50%. IR: 2923 (s), 2854 (s), 2726 (w), 1634(s), 1589(s), 1532 (s), 1463 (s), 1377(s), 1335 (m), 1281 (m), 1240 (m), 1214 (m), 1181 (m), 1104 (m), 1067 (m), 1049 (w), 966 (m), 892 (w), 871 (m), 840 (w), 810 (s), 788 (w), 754 (s), 739 (w), 722 (s), 672 (w), 615 (w), 595 (w), 574 (w), 549 (w), 533 (m), 521 (s), 499 (s), 467 (m). M. S. (MALDI-ToF): 1051 (M-Co-MeCN), 961 (M-Br-

MeCN), 871 (M-Br_3-MeCN), 855 (M-$CoBr_3$), 818 (M-anion), 738 (M-Br - anion). Mag moment: μ_{eff} 6.77 B.M.

Synthesis of [CoBr**L**^{tBu}][$CoBr_3$(NCMe)]·0.5MeCN (**1*t*Bu**·0.5MeCN)

L$^{tBu}H_2$ (0.50 g, 0.65 mmol) and $CoBr_2$ (0.29 g, 1.33 mmol) were weighed out in a dry box. After transferring to a Schlenk line, toluene (20 mL) was added and the system was refluxed for 12 h. On cooling, the volatiles were removed *in-vacuo*, and the residue was extracted into warm MeCN (20 mL). On cooling (0 ^{o}C), green prisms were formed which were isolated and dried *in-vacuo* to afford **1*t*Bu**·0.5MeCN (1.13 g, 69% yield). Elemental analysis calculated for $C_{110}H_{106}Br_8Co_4N_{11}O_4$ C 52.40, H 4.24, N 6.11%. Found: C 51.94, H 4.24, N 5.84%. IR: 3534 (w), 3415 (w), 3051 (m), 2925 (s), 2855 (s), 2729 (m), 2307 (m), 2280 (w), 2251 (w), 1973 (w), 1892 (m), 1886 (w), 1633 (s), 1619 (s), 1584 (m), 1558 (w), 1537 (s), 1502 (w), 1484 (m), 1462 (s), 1395 (s), 1377 (s), 1360 (m), 1335 (s), 1299 (m), 1283 (m), 1241 (s), 1218 (s), 1180 (m), 1165 (w), 1159 (w), 1137 (m), 1102 (m), 1063 (s), 1047 (s), 1020 (s), 955 (m), 945 (w), 939 (w), 912 (m), 843 (m), 828 (m), 794 (m), 766 (s), 725 (w), 688 (m), 675 (w). M. S. (MALDI-ToF): 1041 [M-(MeCN)-Br_2], 961 [M-(MeCN)-Br_3], 822 [M-Br-anion]. Mag moment: μ_{eff} 6.66 B.M. For [CoBr**L**^{tBu}]$_2$[$CoBr_3$(NCMe)][Br]·4.5MeCN (**2*t*Bu**·4.5MeCN): On concentration of the mother-liquor and further cooling, small red prisms **2*t*Bu**·4.5MeCN were also isolated in low yield (*ca*. 10%). For $C_{115}H_{113.5}Br_6Co_3N_{13.5}O_4$: C 57.43, H 4.76, N 7.86%; found: C 57.79, H 4.67, N 6.44%. IR: 2957 (s), 2924 (s), 2854 (s), 2728 (m), 1633 (m), 1584 (m), 1537 (m), 1462 (s), 1261 (s), 1094 (s), 1020 (s), 875 (m), 799 (s), 757 (w), 722 (m), 660 (w), 598 (w), 540 (w), 466 (w). M. S. (ToF ASAP+): 904 (M^+), 822 (M^+ - Br).

Synthesis of [ZnBr**L**^{Me}][$ZnBr_3$(NCMe)]·MeCN (**3Me**·MeCN)

As for **1Me**·4MeCN, but using $L^{Me}H_2$ (0.50 g, 0.73 mmol) and $ZnBr_2$ (0.30 g, 1.33 mmol) affording yellow prisms of **3Me**·MeCN. Yield 0.53 g, 61%. Elemental analysis calculated for $C_{50}H_{46}Br_4N_6O_6Zn_2$-MeCN: C

49.26, H 3.53, N 5.98%; found: C 49.02, H 3.32, N 6.06 %. IR (KBr) cm^{-1}: 2918 (s), 2853 (s), 2727 (m), 2672 (m) , 2349 (w), 1727 (w), 1709 (w), 1692 (w) , 1633 (m), 1591 (m), 1532 (m), 1299 (m), 1280 (m), 1261 (s), 1212 (w), 1196 (w), 1180 (m), 1154 (m), 1101 (s), 1066 (m), 1019 (m), 891 (w), 872 (w), 801 (s), 754 (m), 722 (s), 671 (w), 659 (w), 595 (w), 574 (w), 531 (w), 496 (w), 464 (w). M. S. (MALDI-ToF): 825 (M-anion), 765 (M-Br-anion) 681 (M-ZnBr-anion). ^{1}H NMR (CD_3CN, 400 MHz): δ 8.63 (d, 2H, J=13.2, Ar-*H*), 8.40 (s, 2H, C*H*=N), 7.63 (d, 2H, J=2.0, Ar-*H*), 7.52 (m, 8H, Ar-*H*), 6.95 (m, 6H, Ar-*H*), 6.76 (td, 6H, J_1=8.0, J_2=2.0, Ar-*H*), 6.21 (d, 2H, J=7.2, C*H*=N), 3.72 (t, 2H, J=14.8, CH_2), 3.45 (dt, 2H, J_1=14.4, J_2=3.6, CH_2), 2.99 (dt, 2H, J_1=14.8, J_2=4.8, CH_2), 2.56 (td, 2H, J_1=13.4, J_2=3.2, CH_2), 2.26 (s, 6H, CH_3).

Synthesis of [ZnBr**L**$^{t\mathbf{Bu}}$][$ZnBr_3$(NCMe)]·MeCN (**3*t*Bu**·MeCN)

As for **1*t*Bu**·0.5MeCN, but using $L^{t\mathrm{Bu}}H_2$ (0.50 g, 0.65 mmol) and $ZnBr_2$ (0.30 g, 1.33 mmol) affording yellow prisms of **3*t*Bu**·MeCN. Yield 0.62 g, 76%. Elemental analysis calculated for $C_{54.25}H_{55}Br_4N_5O_{2.25}Zn_2$: C 51.63 H 4.39 N 5.54%; found: C 51.50, H 4.41, N 5.67%. IR: 2956 (s), 2924 (s), 2854 (s), 2728 (m), 2349 (w), 2293 (m), 1634 (s), 1621 (s), 1587 (s), 1574 (w), 1556 (w), 1535 (s), 1502 (w), 1480 (m), 1463 (s), 1396 (m), 1377 (s), 1366 (m), 1329 (s), 1297 (w), 1284 (w), 1260 (m), 1240 (s), 1217 (m), 1182 (m), 1154 (m), 1101 (m), 1060 (m), 1048 (w), 1021 (m), 953 (w), 934 (w), 909 (w), 890 (m), 877 (w), 841 (w), 794 (s), 754 (s), 723 (m), 688 (w). M. S. (MALDI-ToF): 909 [M-anion], 827 [M-Br-anion], 765.4 [M-ZnBr-anion]. ^{1}H NMR (CD_3CN, 400 MHz): δ 8.70 (d, 2H, J=13.2, Ar-*H*), 8.50 (s, 2H, C*H*=N), 7.94 (d, 2H, J=2.8, Ar-*H*), 7.70 (d, 2H, J=2.8, Ar-*H*), 7.54 (m, 6H, Ar-*H*), 7.01 (d, 2H, J=6.8, Ar-*H*), 6.95 (td, 2H, J_1=8.0, J2=1.2, Ar-*H*), 6.78 (td, 2H, J_1=7.6, J_2=2.4, Ar-*H*), 6.23 (d, 2H, J=6.4, C*H*=N), 3.71 (t, 2H, J=13.2, CH_2), 3.52 (dt, 2H, J_1=14.0, J_2=4.4, CH_2), 3.01 (dt, 2H, J_1=14.4, J_2=4.0, CH_2), 2.58 (td, 2H, J_1=13.6, J_2=3.2, CH_2), 2.11 (s, 18H, C(CH_3)$_3$).

Synthesis of [CoBr**L**^{tBu}]$_2$[$Co_{0.68}Zn_{0.32}Br_3$(NCMe)]·0.25MeCN (**4*t*Bu**·0.25MeCN)

To **1*t*Bu**·0.5MeCN (1.00 g 0.80 mmol) was added $ZnBr_2$ (0.18 g, 0.80 mmol) and the system was refluxed for 12 h. On cooling, the volatiles were removed *in vacuo* and the residue was extracted into MeCN (30 mL). Prolonged standing at ambient temperature afforded green/brown prisms of **4*t*Bu**·0.25MeCN. Yield 0.53 g, 53%. Elemental analysis calculated for $C_{54.50}H_{55}Br_4N_{5.25}O_2Co_{1.68}Zn_{0.32}$: C 52.15 H 4.41 N 5.86%, C 52.34, H 4.56, N 5.85%. IR (KBr) cm^{-1}: 2955 (s), 2925 (s), 2854 (s), 2727 (w), 2305 (w), 1748 (w), 1632 (s), 1618 (s), 1537 (s), 1462 (s), 1395 (w), 1377 (s), 1366 (m), 1299 (w), 1260 (s), 1217 (w), 1180 (m), 1101 (s), 1063 (s), 1020 (s), 884 (m), 798 (s), 757 (m), 723 (m), 688 (m), 598 (m), 576 (m), 540 (m), 497 (m), 476 (w). M.S. (ASAP, positive mode): 1135 [M – Br - MeCN], 1037 [M - $Zn_{0.33}$ - Br_2 -MeCN], 969 [M - Br_3 - MeCN], 939 [M - $Zn_{0.33}$ - Br_3 - MeCN], 904 [M - anion], 822 [M - Br-anion].

Synthesis of [Co**L**^{Me}(NCMe)(μ-Br)ZnBr]·3MeCN (**5Me**·3MeCN)

To **1Me**·4MeCN (1.00 g, 0.76 mmol) in THF (30 mL) at -78 °C was added Me_2Zn (0.76 mL, 1.0 M, 0.76 mmol) and the system was slowly allowed to warm to ambient temperature and left to stir for 12 h. Volatiles were then removed *in-vacuo*, and the residue was extracted in MeCN (20 mL). Cooling to 0 °C afforded large red/brown prisms of **5Me**·3MeCN (-3MeCN, sample dried in vacuo for 12h). Yield: 0.42 g, 49%. Further crops of **5Me**·3MeCN can be obtained from the mother-liquor (total isolated yield 61%). Elemental analysis calculated for $C_{48}H_{41}Br_2CoN_5O_2Zn$: C 57.42, H 4.12, N 6.98%. Found: C, 57.20, H 3.95, N 7.13%. IR (KBr) cm^{-1}: 2922 (s), 2853 (s), 1634 (s), 1589 (s), 1535 (s), 1463 (s), 1377 (s), 1341 (s), 1297 (s), 1104 (s), 1069 (s), 1041 (s), 1017 (s), 919 (s), 869 (s), 839 (s), 801 (s), 754 (m), 740 (w), 722 (m), 672 (m), 615 (w), 597 (w), 574 (w), 554 (w), 533 (m), 521 (w), 499 (m), 467 (m). M. S. (MALDI-ToF): 962 [M-4MeCN]. Mag moment: μ_{eff} 5.10 B.M. [4]

Synthesis of [Co**L**^{tBu}(NCMe)(μ-Br)ZnBr]·3.25MeCN (**5*t*Bu**·3.25MeCN)

To **1*t*Bu**·0.5MeCN (1.00 g, 0.80 mmol) in THF (30 mL) at -78 ^{o}C was added Et_2Zn (0.66 mL, 1.2 M, 0.80 mmol) and the system was slowly allowed to warm to ambient temperature and left to stir for 12 h. Volatiles were then removed *in-vacuo*, and the residue was extracted in MeCN (20 mL). Cooling to 0 ^{o}C afforded large red/brown prisms of **5*t*Bu**·3.25MeCN. Yield: 0.64 g, 66%. Elemental analysis calculated for $C_{242}H_{251}Br_8Co_4N_{33}O_8Zn_4$: C 59.49, H 5.18, N 9.46%. found: C 59.74, H 4.89, N 9.30%. IR (KBr) cm^{-1}: 2925 (s), 2855 (s), 2726 (w), 2304 (w), 2275 (w), 2246 (w), 1615 (s), 1591 (m), 1537 (m), 1464 (s), 1378 (m), 1332 (m), 1311 (m), 1287 (w), 1263 (m), 1248 (w), 1234 (w), 1211 (m), 1187 (m), 1156 (w), 1141 (w), 1125 (w), 1088 (w),1059 (m), 1034 (w), 1023 (w), 1013 (w), 982 (m), 964 (w), 917 (w), 895 (w), 863 (w), 799 (w), 774 (m), 754 (m), 739 (m), 726 (m), 690 (w), 655 (w), 631 (w), 581 (w), 553 (w), 525 (m), 507 (m), 482 (m), 466 (w). M. S. (MALDI-ToF): 1041 [M-5MeCN], 961 [M-Br-5MeCN], 822 [M-$ZnBr_2$-5MeCN], 766 [M-$ZnCoBr_2$-5MeCN]. Mag moment: μ_{eff} 5.23 B.M. [4]

Ring opening polymerization

Typical polymerization procedures are as follows. A toluene solution of **5** (0.010 mmol, in 1.0 mL toluene) was added into a Schlenk tube in the glove-box at room temperature. The solution was stirred for 2 min, and then 1 or 2 equivalent of BnOH (from 1 mmol BnOH in 100 mL toluene) and the appropriate amount of *ε*-CL or δ-VL (e.g. 2.5 mmol) along with 1.5 mL toluene was added to the solution. The reaction mixture was then placed into an oil bath pre-heated to the required temperature, and the solution was stirred for the prescribed time. The polymerization mixture was then quenched by addition of an excess of glacial acetic acid (0.2 mL) into the solution, and the resultant solution was then poured into cold methanol (200 mL). The resultant polymer was then collected on filter paper and was dried *in vacuo*.

Co-polymerizations

Synthesis of co-polymer (δ-VL+ ε-CL):

A toluene solution of **5*t*Bu** (0.010 mmol, in 1.0 mL toluene) was added into a Schlenk tube in the glove-box at room temperature. The solution was stirred for 2 min, and then 1 equivalent of BnOH (from 1 mmol BnOH in 100 mL toluene) and 5 mmol of δ-VL were added, after 24h *ε*-CL was added to the solution. The reaction mixture was then placed into an oil bath pre-heated to the 130 °C, and the solution was stirred for another 24h. The polymerization mixture was then quenched by addition of an excess of glacial acetic acid (0.2 mL) into the solution, and the resultant solution was then poured into cold methanol (200 mL). The resultant polymer was then collected on filter paper and was dried *in vacuo*.

Synthesis of co-polymer (ε-CL + δ-VL):

A toluene solution of **5*t*Bu** (0.010 mmol, in 1.0 mL toluene) was added into a Schlenk tube in the glove-box at room temperature. The solution was stirred for 2 min, and then 1 equivalent of BnOH (from 1 mmol BnOH in 100 mL toluene) and 5 mmol *ε*-CL of were added, after 24h δ-VL was added to the solution. The reaction mixture was then placed into an oil bath pre-heated to the 130 °C, and the solution was stirred for another 24h. The polymerization mixture was then quenched by addition of an excess of glacial acetic acid (0.2 mL) into the solution, and the resultant solution was then poured into cold methanol (200 mL). The resultant polymer was then collected on filter paper and was dried *in vacuo*.

Synthesis of co-polymer (ε-CL+*r*-LA):

A toluene solution of **5*t*Bu** (0.010 mmol, in 1.0 mL toluene) was added into a Schlenk tube in the glove-box at room temperature. The solution was stirred for 2 min, and then 1 equivalent of BnOH (from 1 mmol BnOH in 100 ml toluene) and 5 mmol *ε*-CL of were added, after 24h *r*-LA was added to the solution. The reaction mixture was then placed into an oil bath pre-heated to the 130 °C, and the

solution was stirred for another 24h. The polymerization mixture was then quenched by addition of an excess of glacial acetic acid (0.2 mL) into the solution, and the resultant solution was then poured into cold methanol (200 mL). The resultant polymer was then collected on filter paper and was dried *in vacuo*.

Kinetic studies

The polymerizations were carried out at 130 ^{o}C in toluene (2 mL) using 0.010 mmol of complex. The molar ratio of monomer to initiator was fixed at 500:1, and at appropriate time intervals, 0.5 µL aliquots were removed (under N_2) and were quenched with wet $CDCl_3$. The percent conversion of monomer to polymer was determined by ^{1}H NMR spectroscopy.

Mass Spectrometry

PVL and co-polymer samples were run at the University of Hull using MALDI-TOF MS analysis. Samples were dissolved in THF, and the matrix, 2-(4-hydroxyphenylazo) benzoic acid (HPABA) with added NaOAc was employed, which was dissolved in THF to give a saturated solution. 50 µL of the sample solution was then mixed with 50µL matrix solution, and 1µL of the mixed solution applied to the sample target. The sample was allowed to dry in air before analysis. The PCL samples were tested at the EPSRC National Mass Spectrometry Service (Swansea), by MALDI ToF in both positive-linear and reflectron modes using a dithranol matrix and NaOAc as additive.

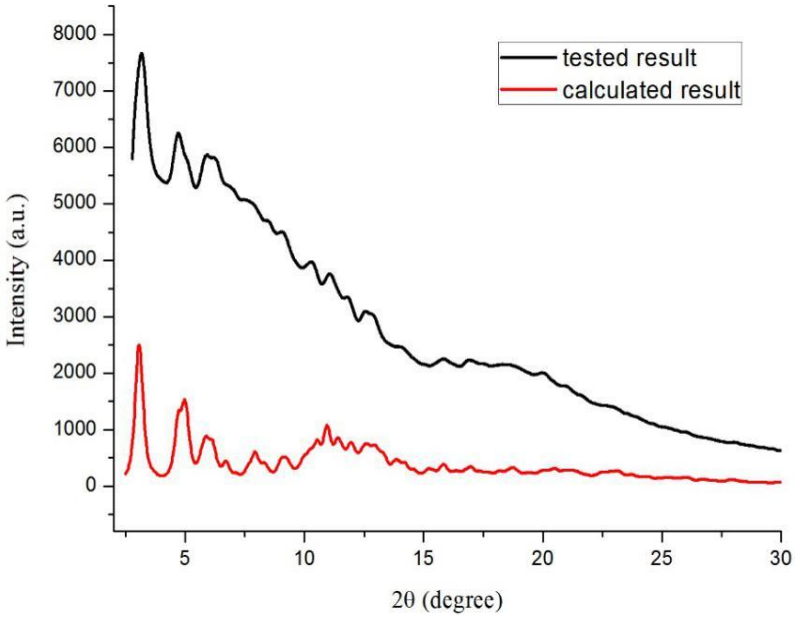

Figure S8. X-ray diffraction data collected from a polycrystalline sample of complex **1*Me***·4MeCN MeCN using Mo Kα radlated diffraction data from the structure determined by single crystal diffraction.

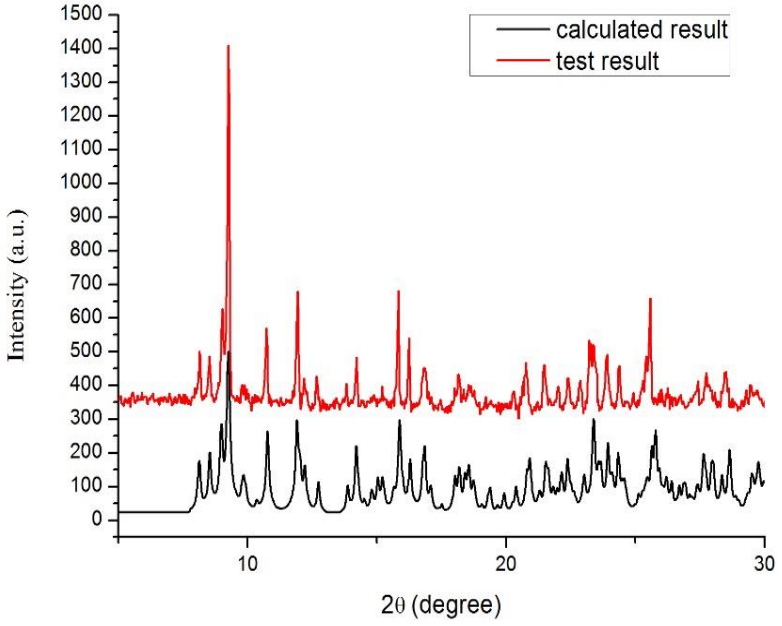

Figure S9. Calculated (black lines) and found powder X-Ray diffraction (PXRD) patterns of [(CoBr**L**$^{t\mathbf{Bu}}$] [$CoBr_3$(NCMe)] ·MeCN (**1*t*Bu**·0.5MeCN).

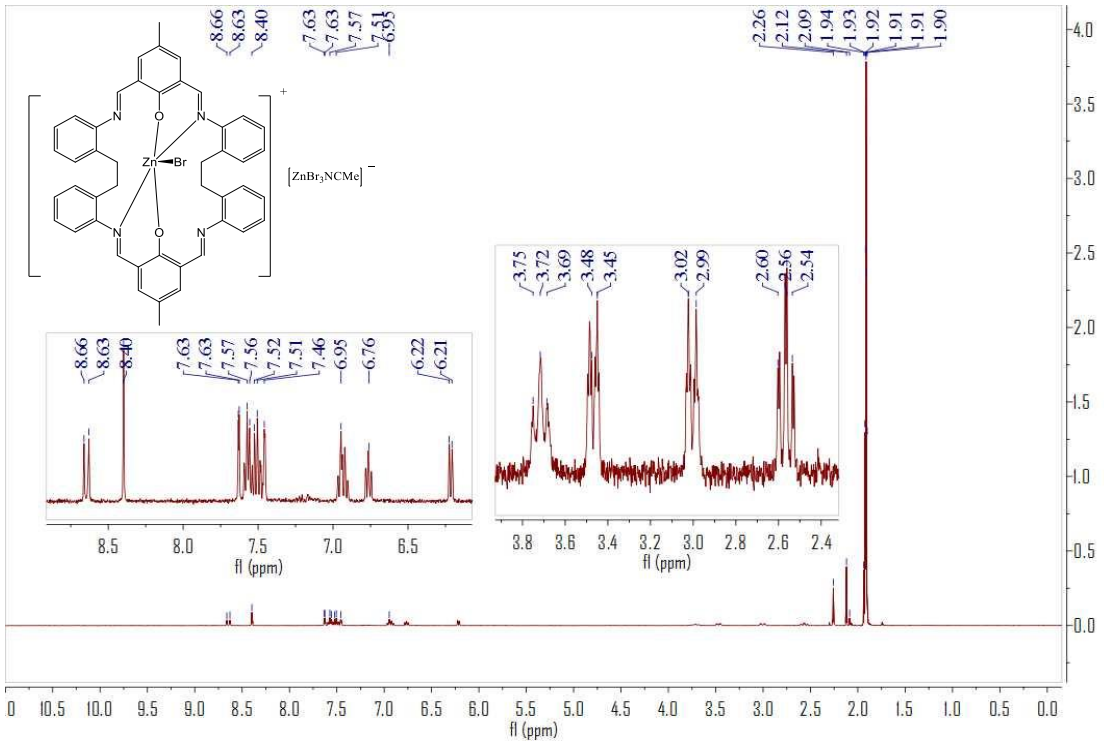

Figure S10. ^{1}H NMR (400 MHz $CDCl_3$) spectrum for **3Me**·MeCN.

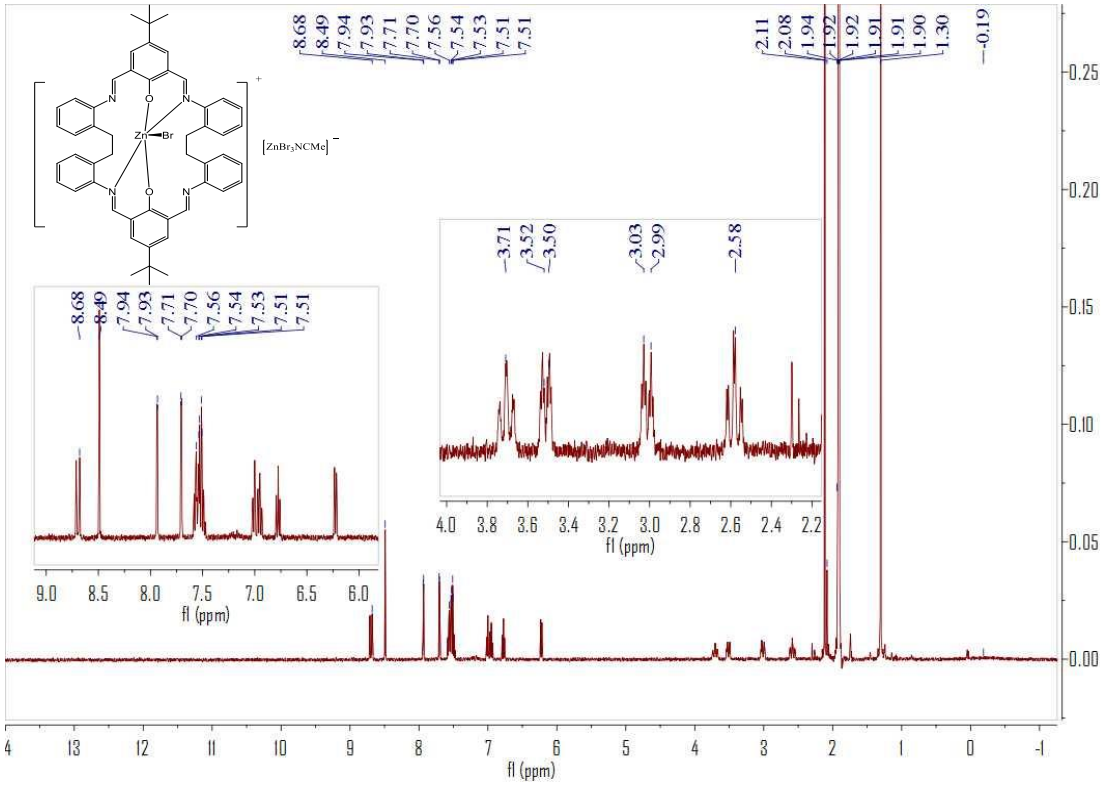

Figure S11. ^{1}H NMR (400 MHz $CDCl_3$) spectrum for **3*t*Bu**·MeCN**.**

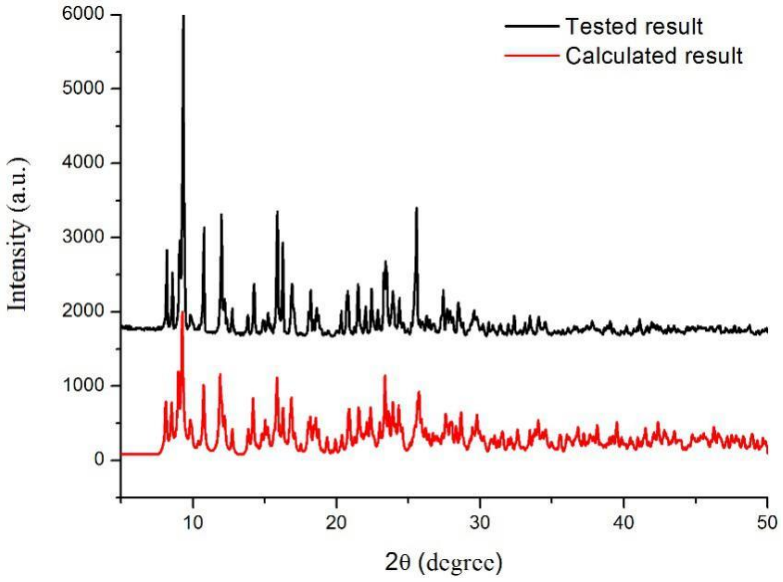

Figure S12. Calculated (black lines) and found powder X-Ray diffraction (PXRD) patterns of [(Zn**L**$^{t\mathbf{Bu}}$Br)][ZnBr$_3$(NCMe)] (**3*t*Bu**·MeCN).

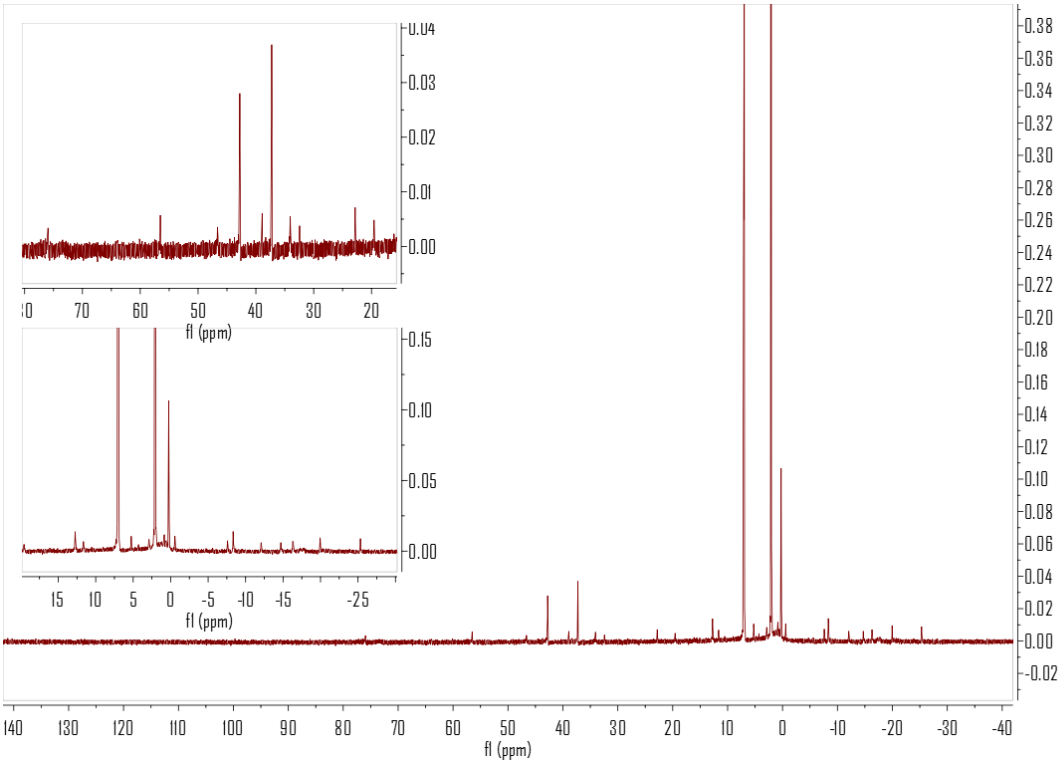

Figure S13. ^{1}H NMR (400 MHz $CDCl_3$) spectrum for **5Me**·3MeCN at 22 °C.

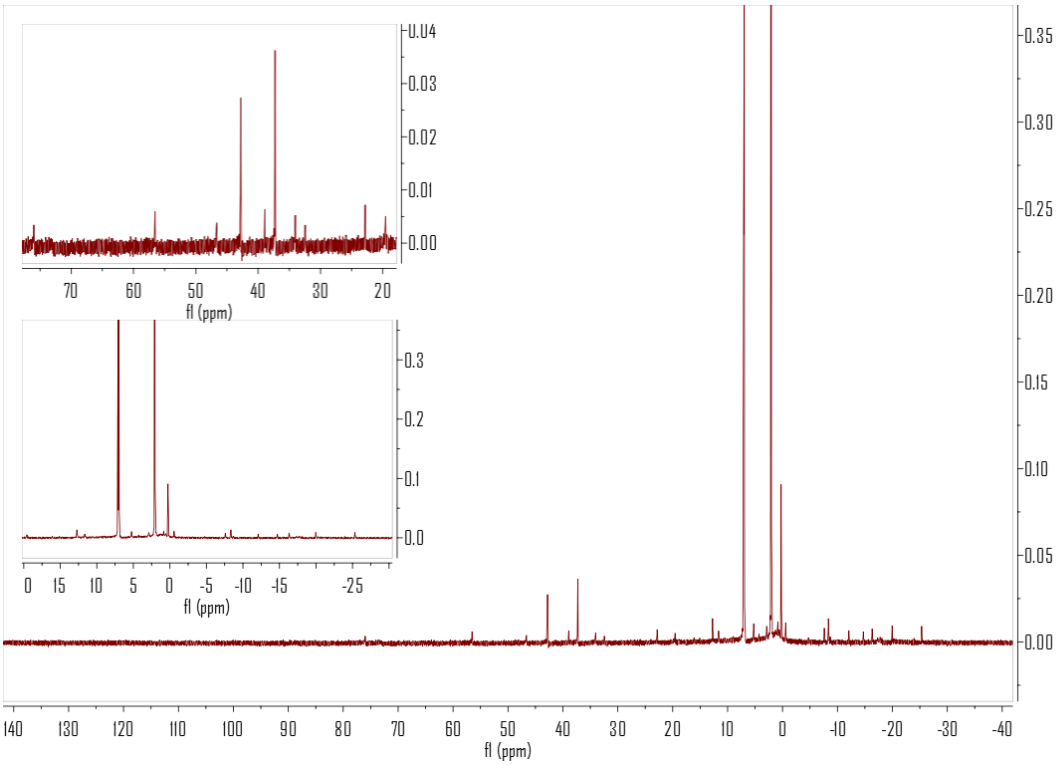

Figure S14. ^{1}H NMR (400 MHz $CDCl_3$) spectrum for **5Me**·3MeCN at 130 °C.

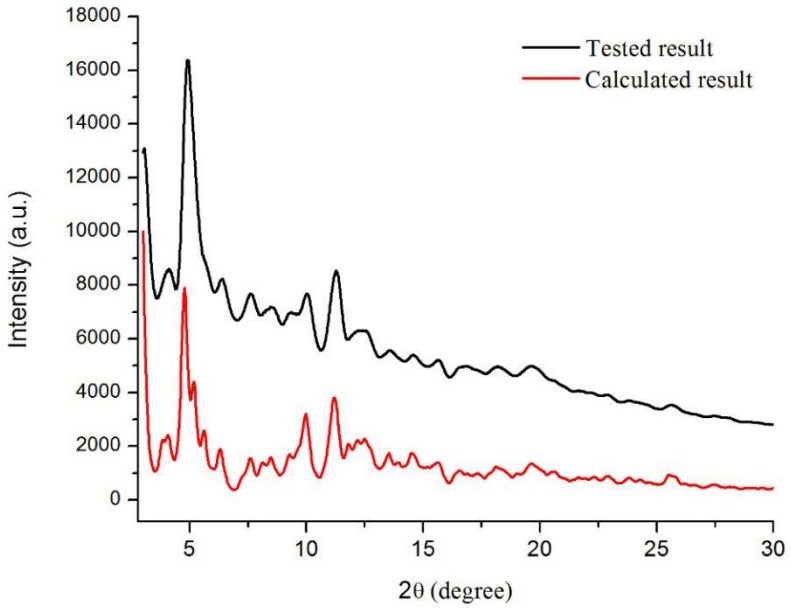

Figure S15. X-ray diffraction data collected from a polycrystalline sample of complex **5Me**·3MeCN using Mo Kα radiation and simulated diffraction data from the structure determined by single crystal diffraction.

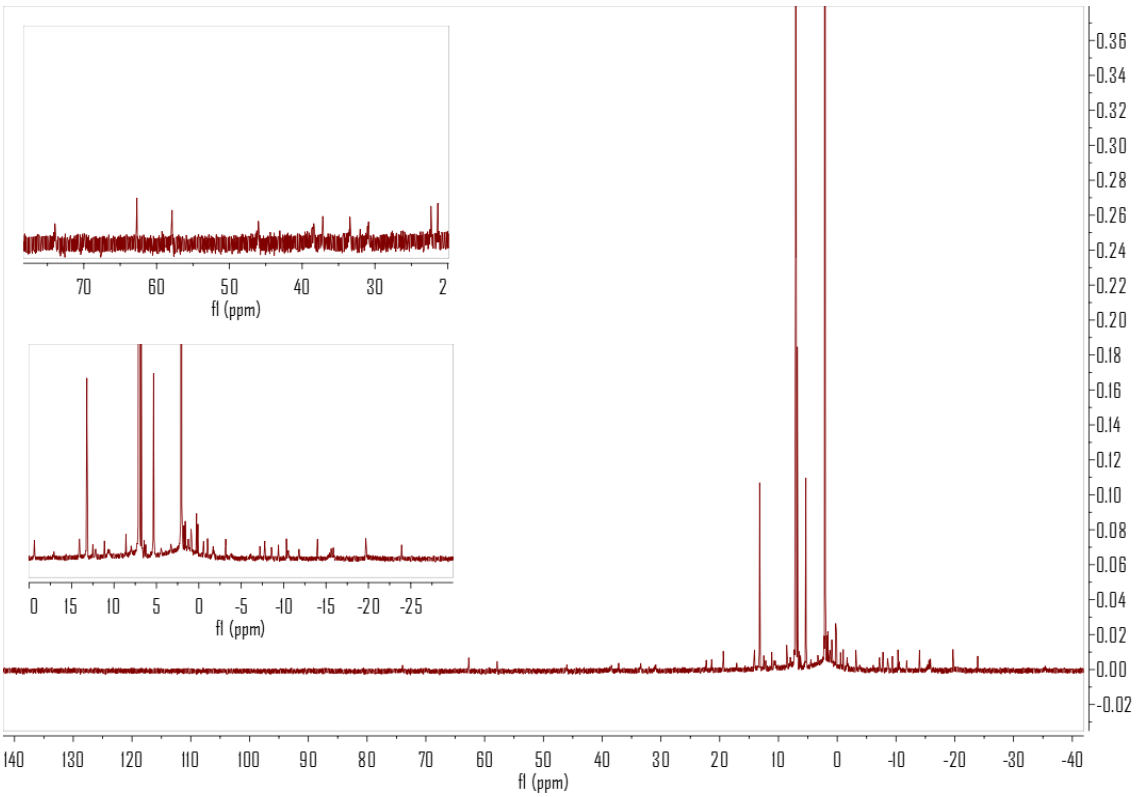

Figure S16. ^{1}H NMR (400 MHz $CDCl_3$) spectrum for **5*t*Bu**·3.25MeCN at 22 °C.

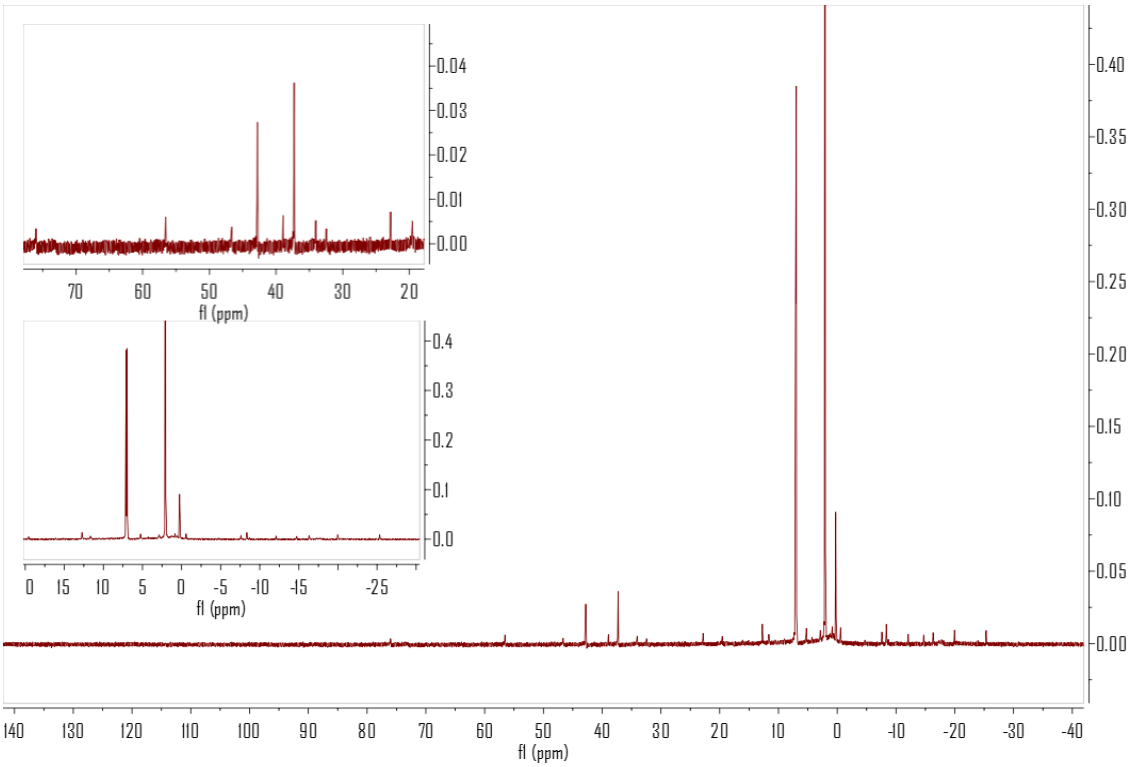

Figure S17. ^{1}H NMR (400 MHz $CDCl_3$) spectrum for **5*t*Bu**·3.25MeCN at 130 °C.

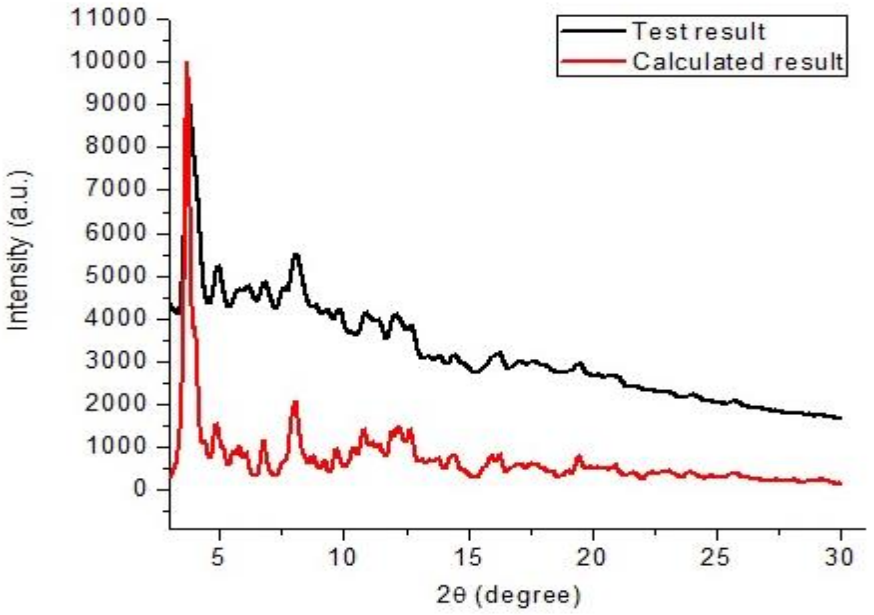

Figure S18. X-ray diffraction data collected from a polycrystalline sample of complex **5*t*Bu**·3.25MeCN MeCN using Mo Kα radlated diffraction data from the structure determined by single crystal diffraction.

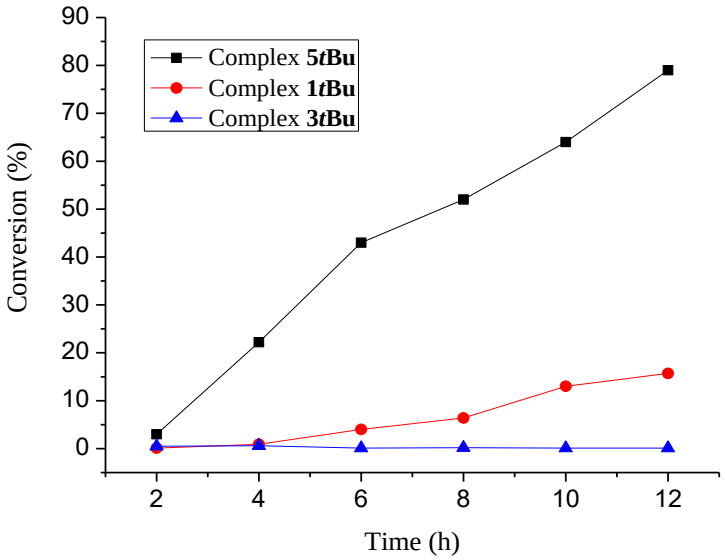

Figure S19. Relationship between conversion and time for the polymerization of δ-VL.

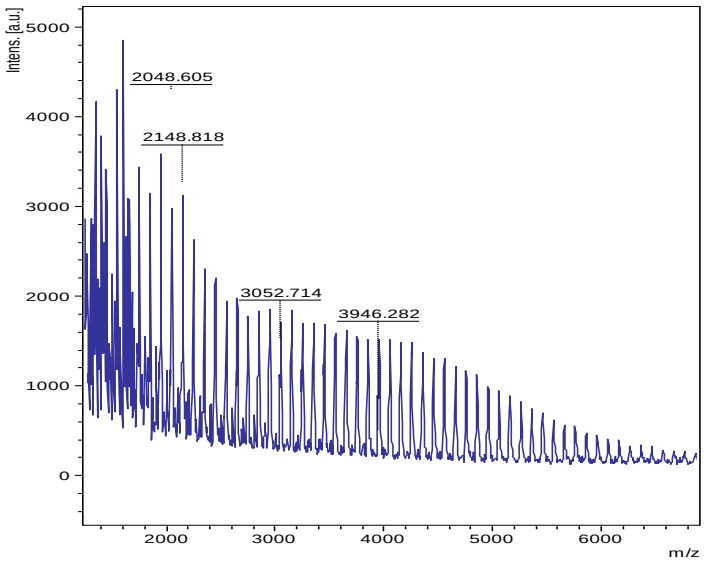

Figure S20. MALDI-ToF mass spectrum for polymer (δ-VL run 4).

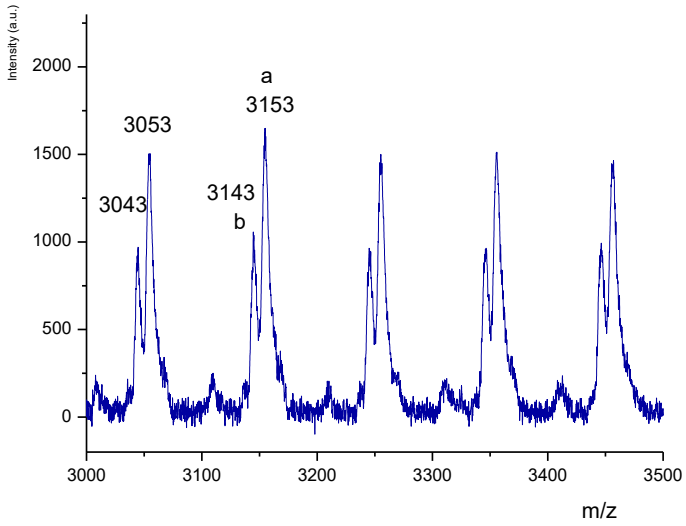

Figure S21. Structure analysis of the polyvalerolactone.

The results indicated that the majority of these polymers were chain-ended by benzyloxy without transesterification [a. M = 108.05 (M_w of BnOH) + n × 100.12 (M_w of VL) + 39.10 (K^+)]. However, a minor series of peaks belonging to PVL chain-ended by hydroxyl group [b. M = 17.01 (M_w of HO) + n × 100.12 (M_w of VL) + 22.99 (Na^+) +1.01 (H)] were observed, which might be caused by traces of water in the monomer. Even after thorough laboratory treatment and with careful handling, liquid monomer VL still

contains traces of water, which has been discussed by some investigators.[5] Neighboring peaks showed a repeat of 100.12 m/z, which agreed with the molecular weight of the VL unit. [6]

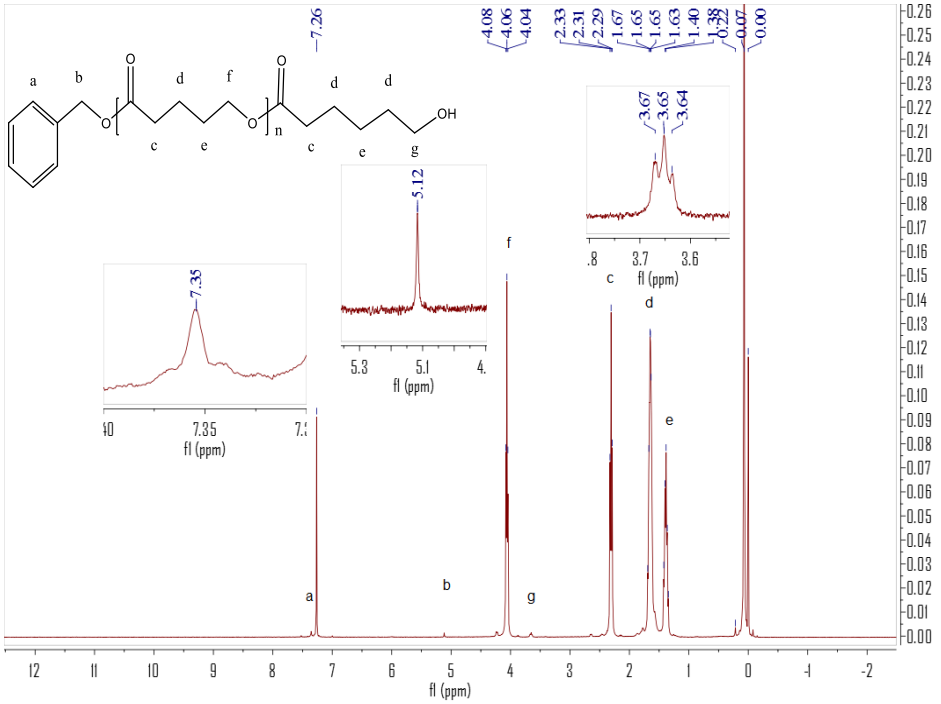

Figure S22. ^{1}H NMR (400 MHz $CDCl_3$) spectrum for polymer (δ-VL run 4). (picture inside is the major product)

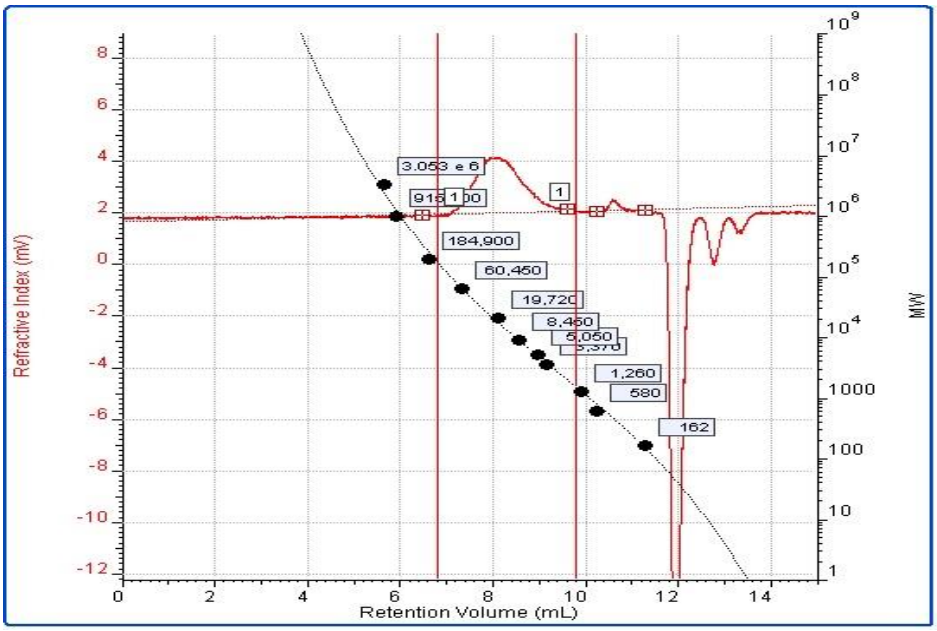

Figure S23. Gel permeation chromatography for δ-VL run 4.

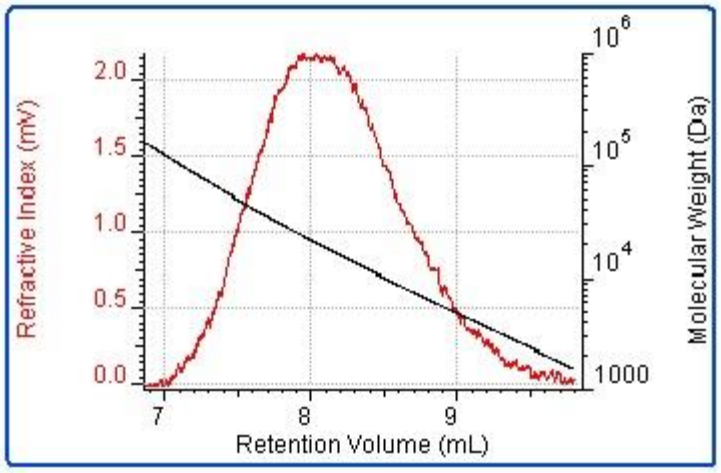

Figure S24. Plot (log M_w) of polyvalerolactone formed for δ-VL run 4.

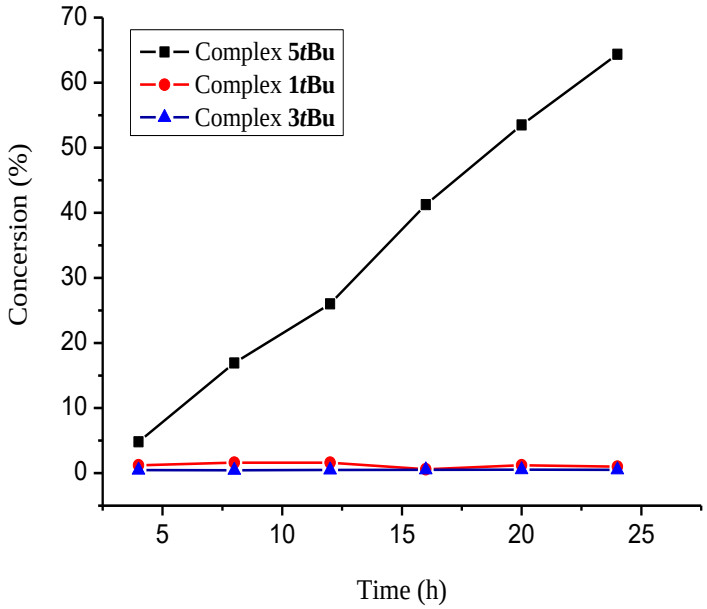

Figure S25. Relationship between conversion and time for the polymerization of ε-CL.

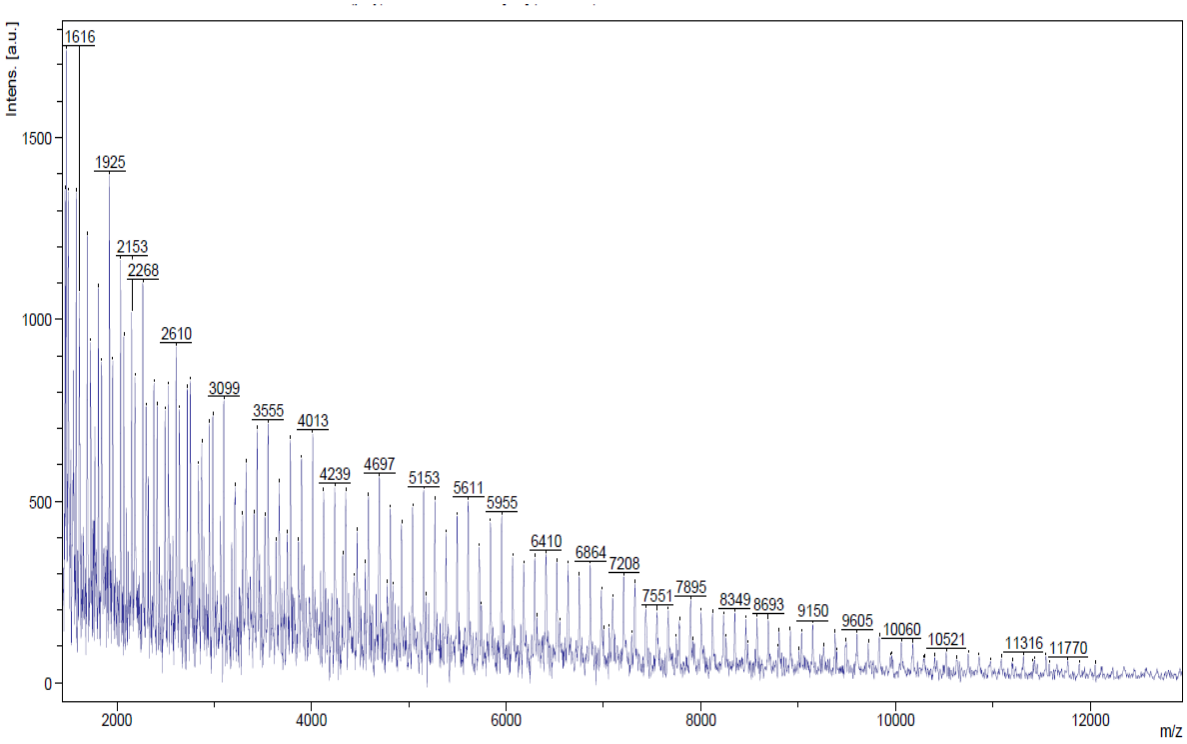

Figure S26. MALDI-ToF mass spectrum for PCL (ε-CL run 4).

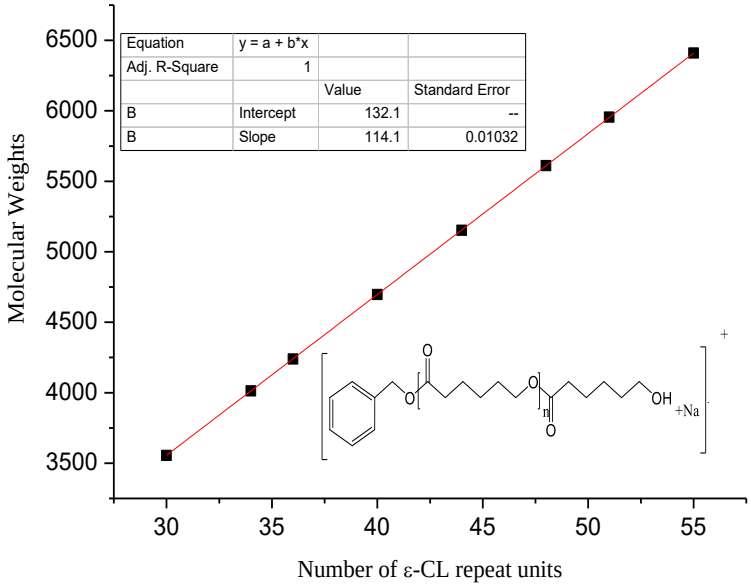

Figure S27. M_w *vs* number of ε-CL repeat units (n) afforded a straight line with a slope of 114.1 and an intercept of 132.1; the slope corresponds to the exact mass of the ε-CL monomer, whereas the intercept corresponds to a polymer chain structure with benzyloxy chain-ends (ε-CL run 4).

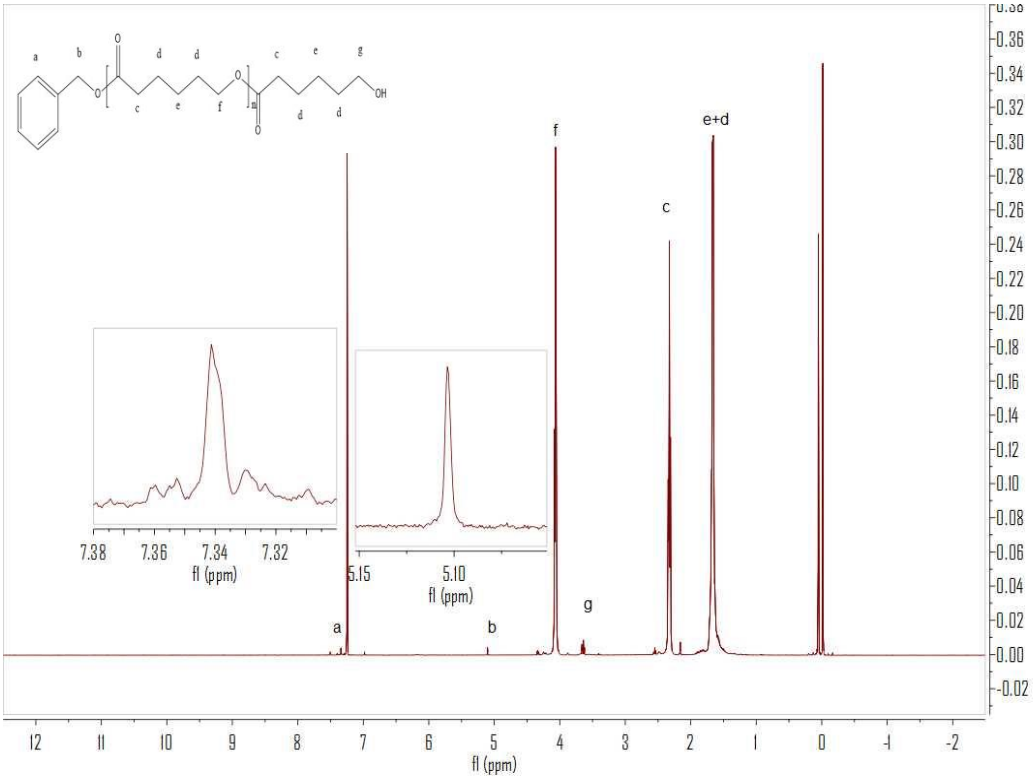

Figure S28. ^{1}H NMR (400 MHz, $CDCl_3$) spectrum for polycaprolactone (ε-CL run 4).

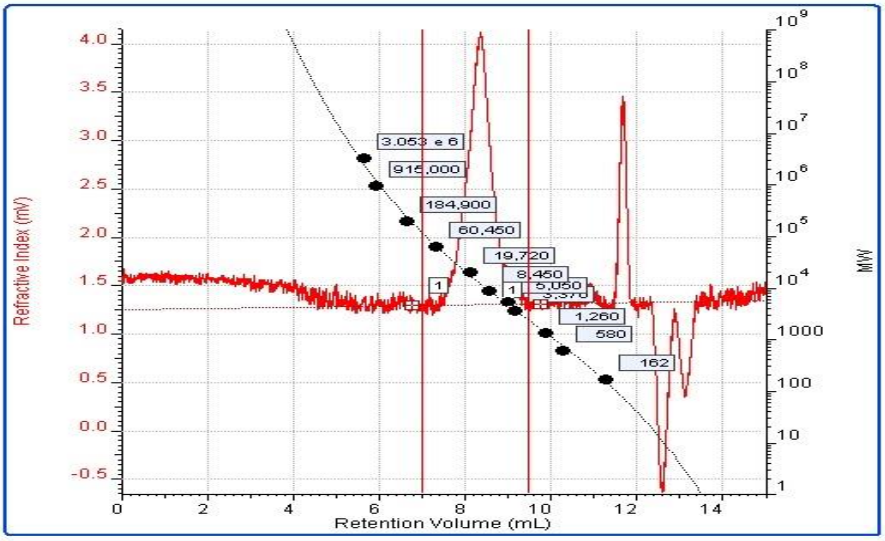

Figure S29. Gel permeation chromatography for ε-CL run 4.

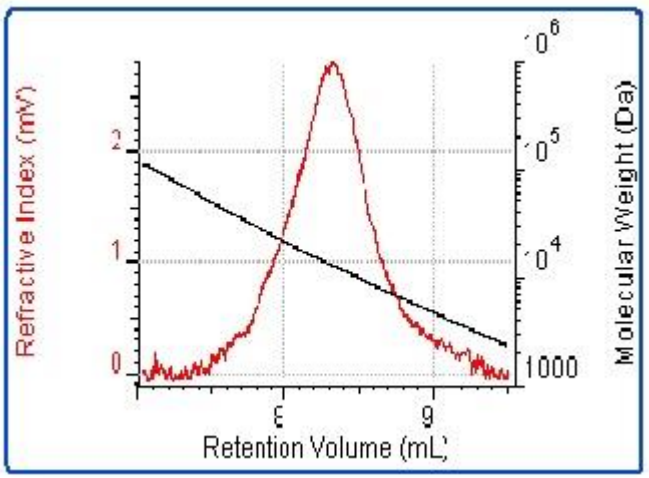

Figure S30. Plot (log M_w) of polycaprolactone formed for ε-CL run 4.

(a)

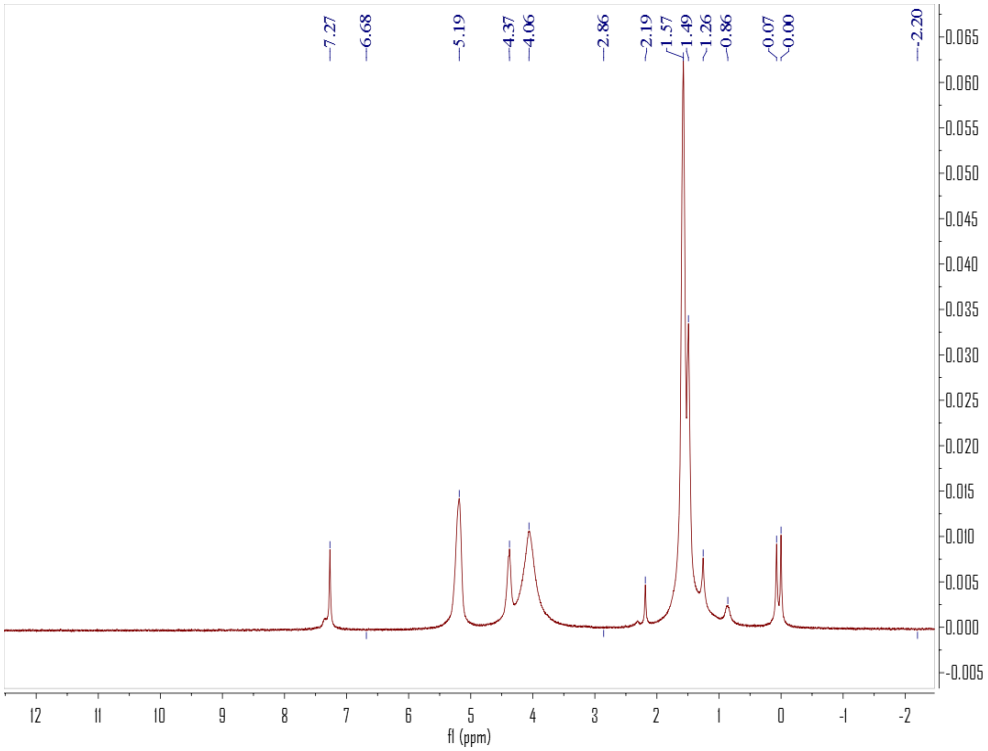

(b)

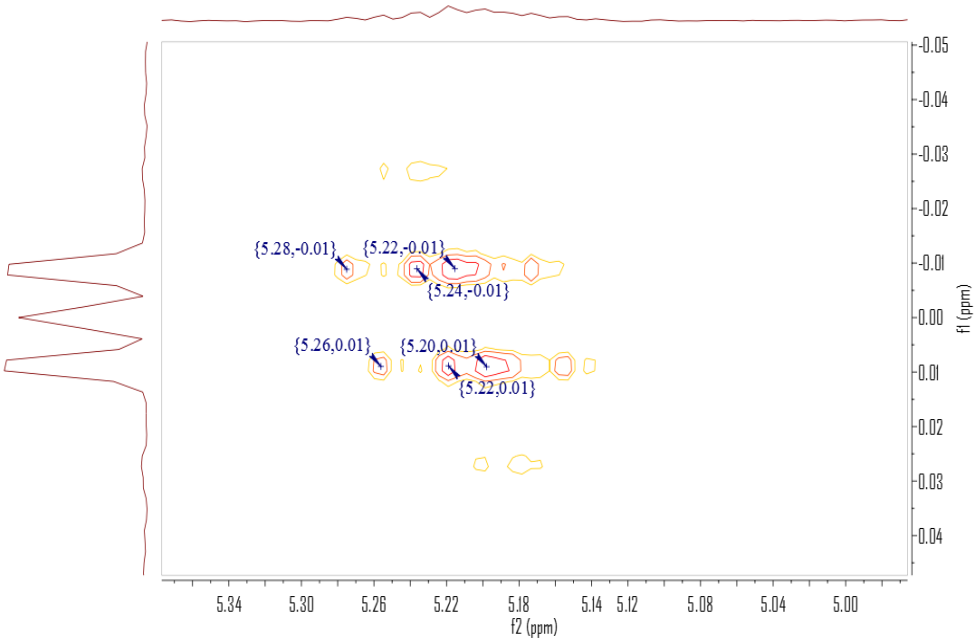

Figure S31. (a). ^{1}H NMR (400 MHz, $CDCl_3$) spectrum for poly(LA). (b). 2D J-resolved ^{1}H NMR spectrum for poly(LA).

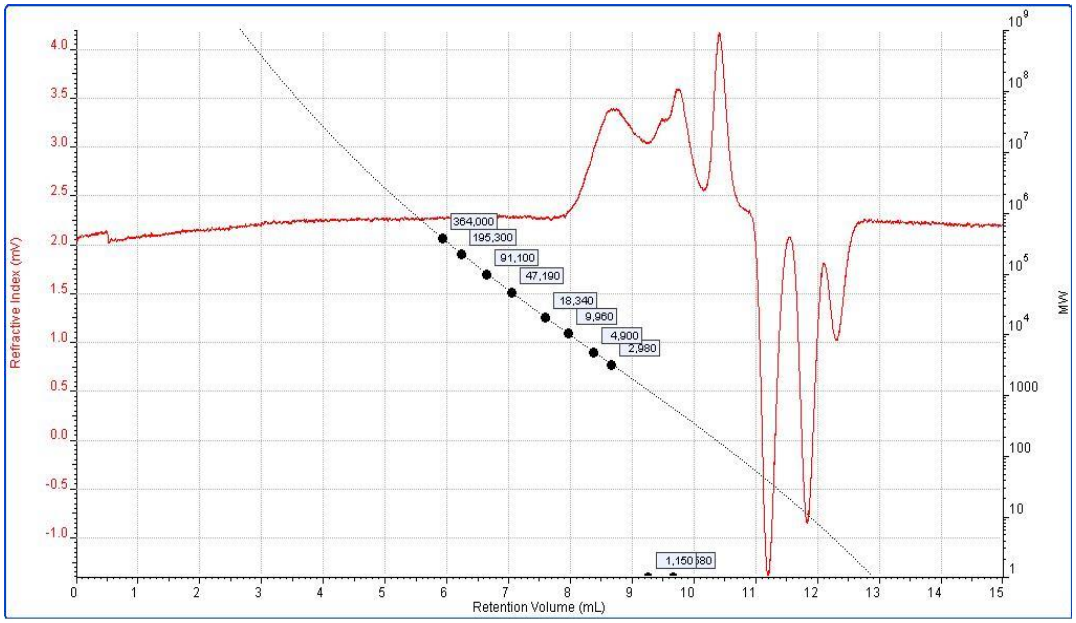

Figure S32. Gel permeation chromatography for poly (LA).

Table S1. Synthesis of block copolymers from cyclic ester monomers using the catalyst **5*t*Bu**.

Run	Composition	t(h)	Incorporated amount	M_n[b]	PDI
1	a. Poly (δ-VL+ ε-CL) [δ-VL]:[ε-CL]:[cat]:[BnOH]= 500:500:1:1	24+24	δ-VL:ε-CL= 51:49	7.29	1.20
2	b. Poly (ε-CL+ δ-VL) [ε-CL]:[δ-VL]:[cat]:[BnOH]= 500:500:1:1	24+24	ε-CL:δ-VL= 47:53	5.37	2.10
3	c. Poly (ε-CL+ *r*-LA) [ε-CL]:[*r*-LA]:[cat]:[BnOH]= 500:500:1:1	24+24	ε-CL: *r*-LA= 61:39	12.55	1.29

[a] Conversion was confirmed by ^{1}H NMR spectroscopy. [b] Determined by GPC analysis calibrated with polystyrene standards and multiplied by correction factor of 0.58.[7]

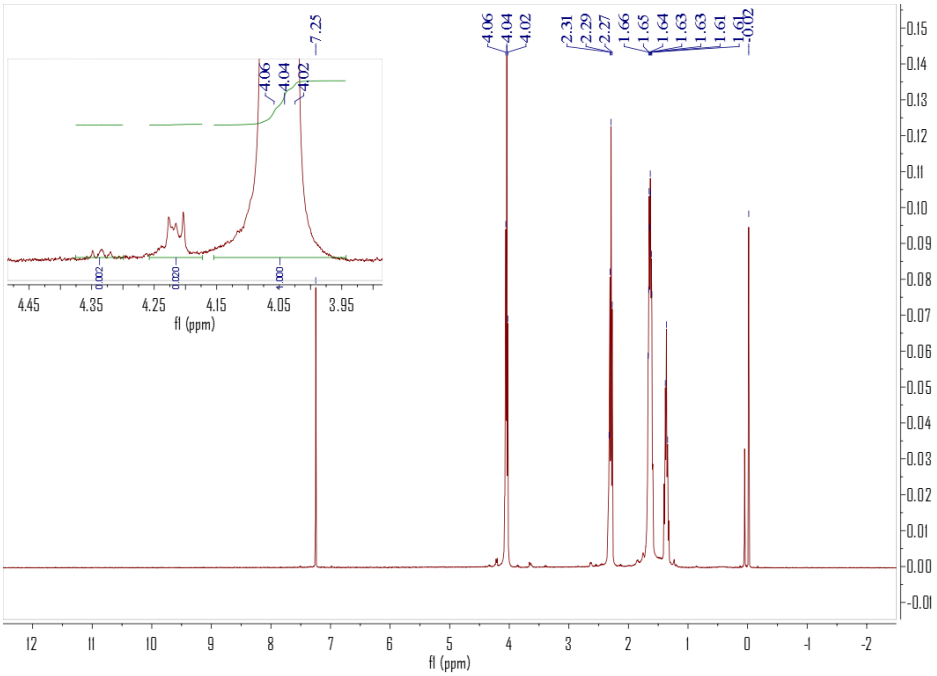

Figure S33. The ^{1}H NMR spectrum of the co-polymer (δ-VL+ ε-CL).

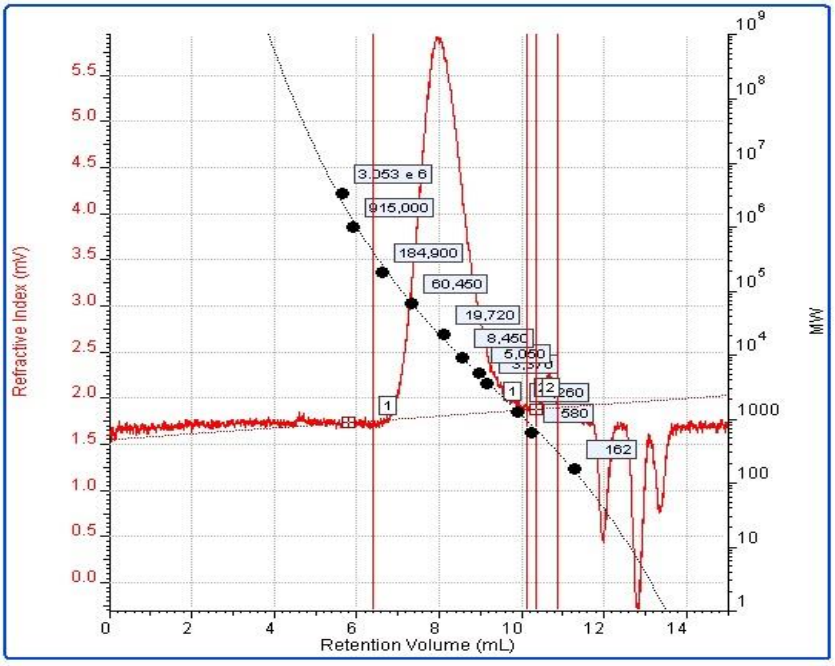

Figure S34. Gel permeation chromatography for co-polymer (δ-VL+ ε-CL).

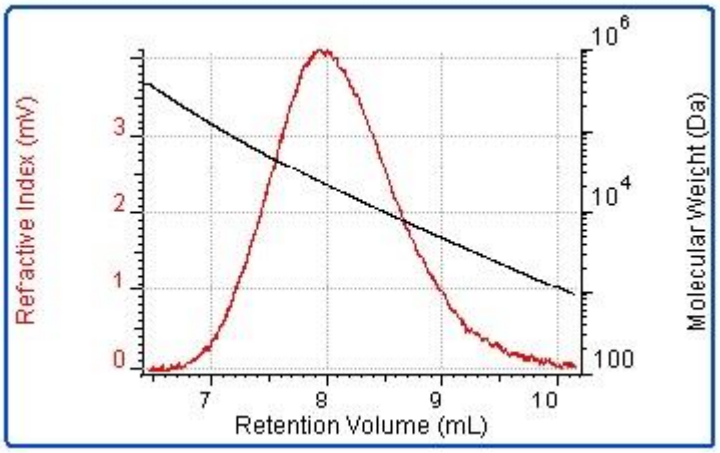

Figure S35. Plot (log M_w) for co-polymer (δ-VL+ ε-CL).

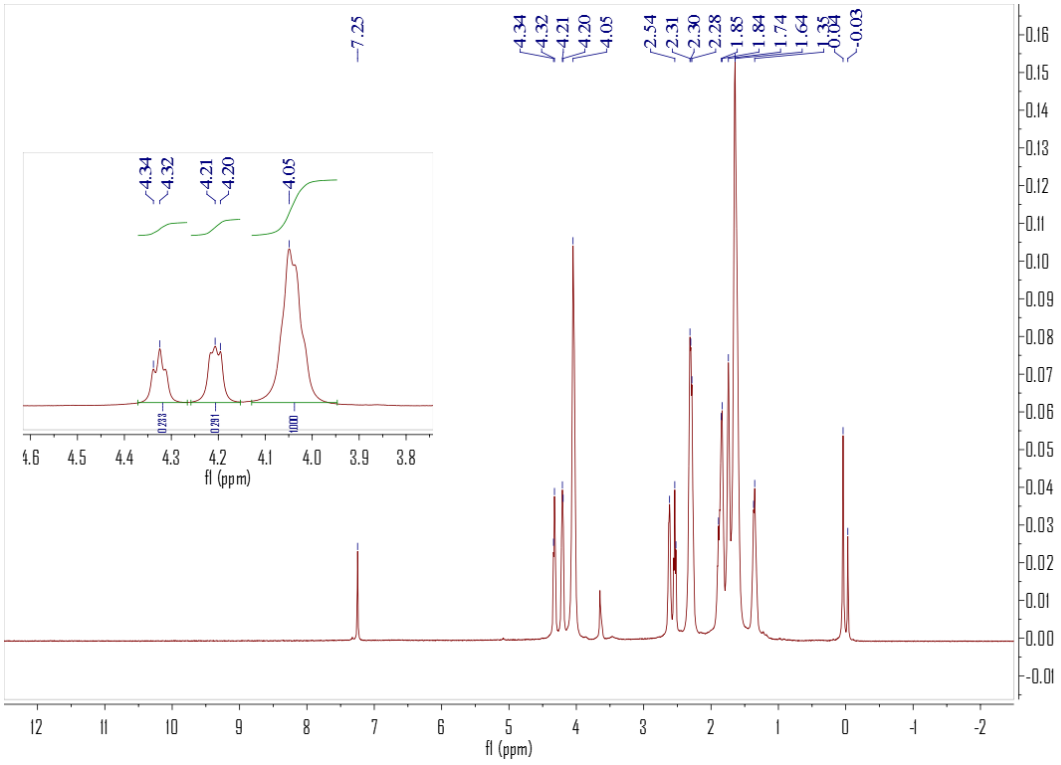

Figure S36. The ^{1}H NMR spectrum of the co-polymer (ε-CL+ δ-VL).

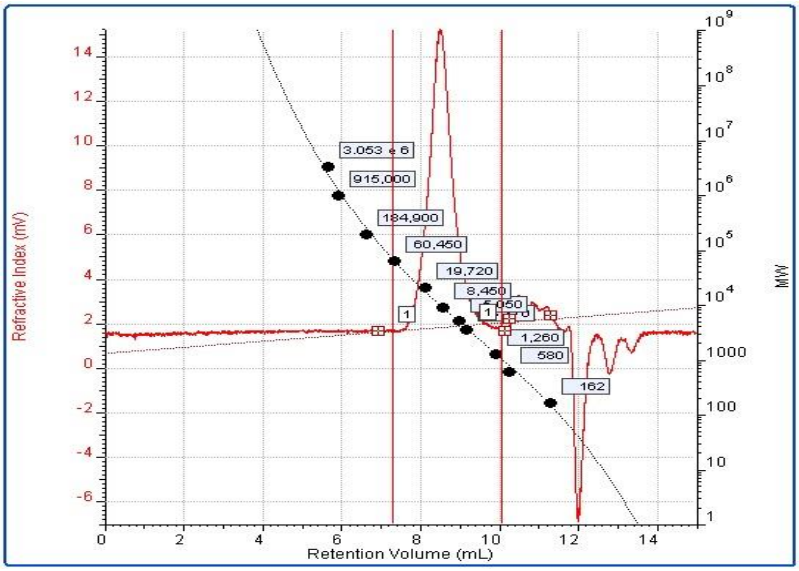

Figure S37. Gel permeation chromatography for co-polymer (ε-CL+ δ-VL).

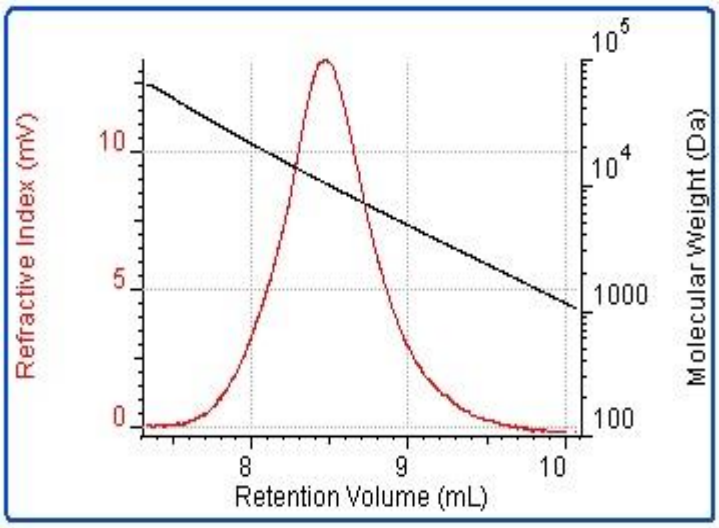

Figure S38. Plot (log M_w) for co-polymer (ε-CL+ δ-VL).

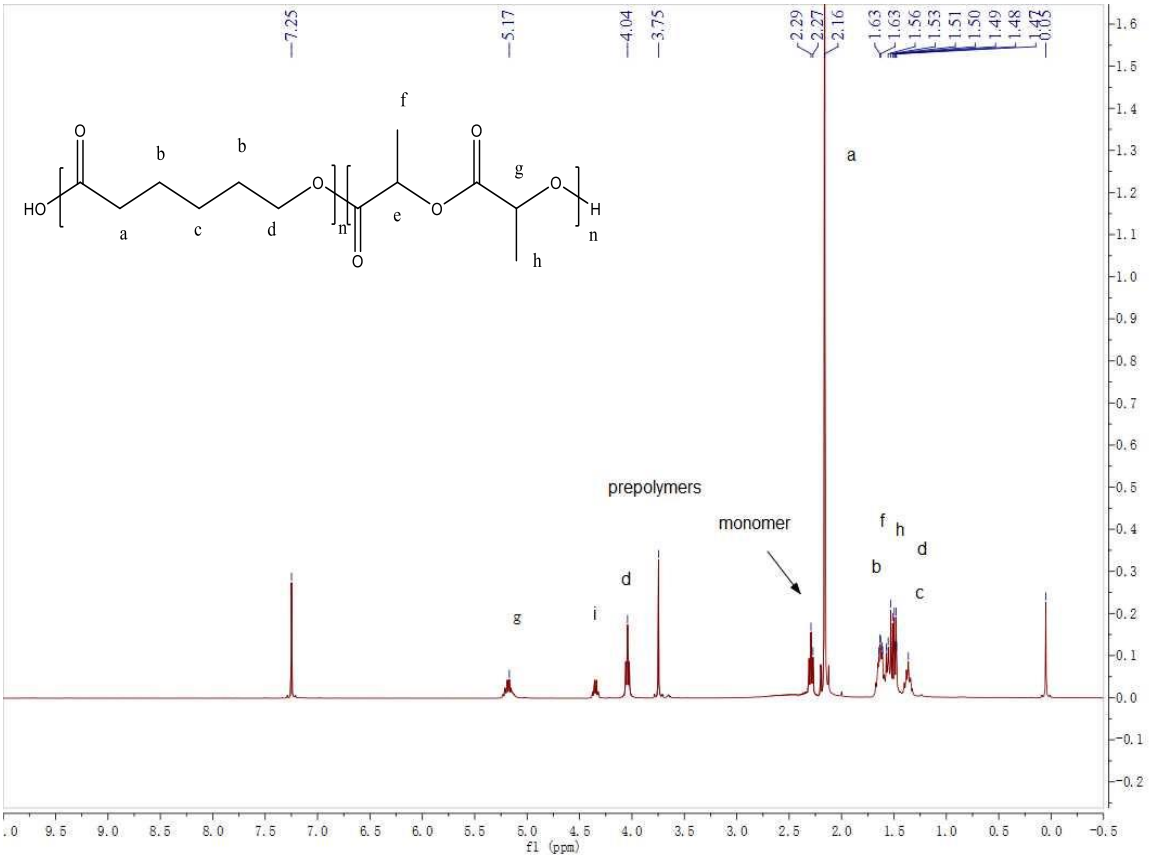

Figure S39. ^{1}H NMR spectrum for co-polymer from co-polymer (ε-CL+ *r*-LA).

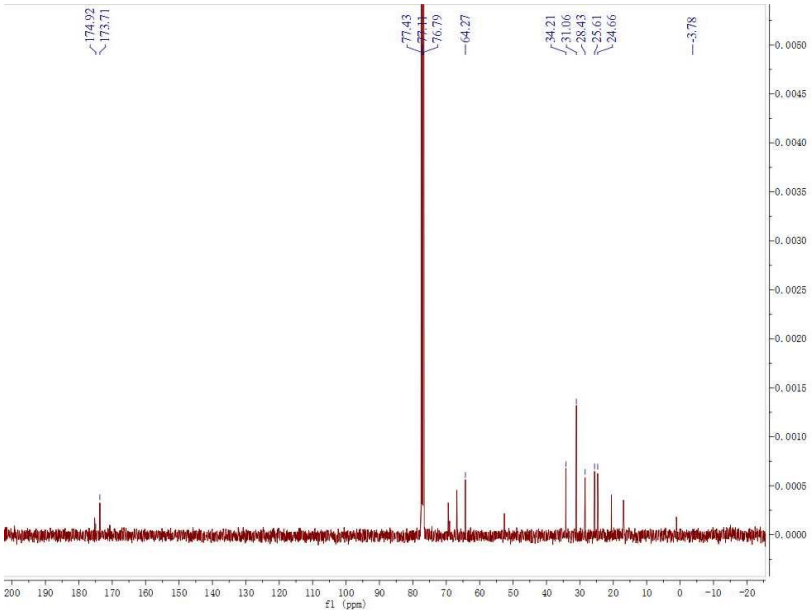

Figure S40. ^{13}C NMR spectrum for co-polymer from ε-CL and *r*-LA.

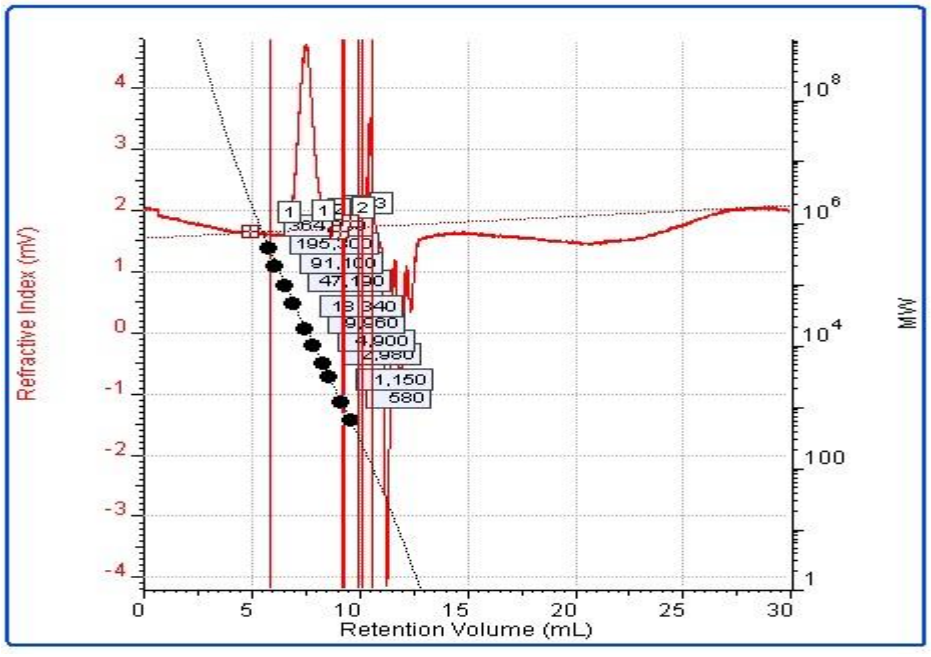

Figure S41. Gel permeation chromatography for co-polymer from ε-CL and *r*-LA.

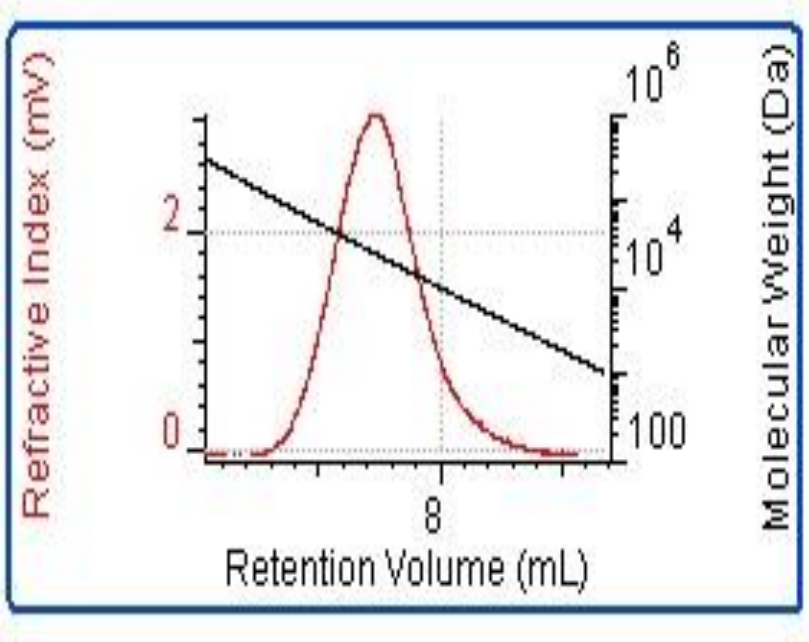

Figure S42. Plot (log M_w) for co-polymer from ε-CL and *r*-LA.

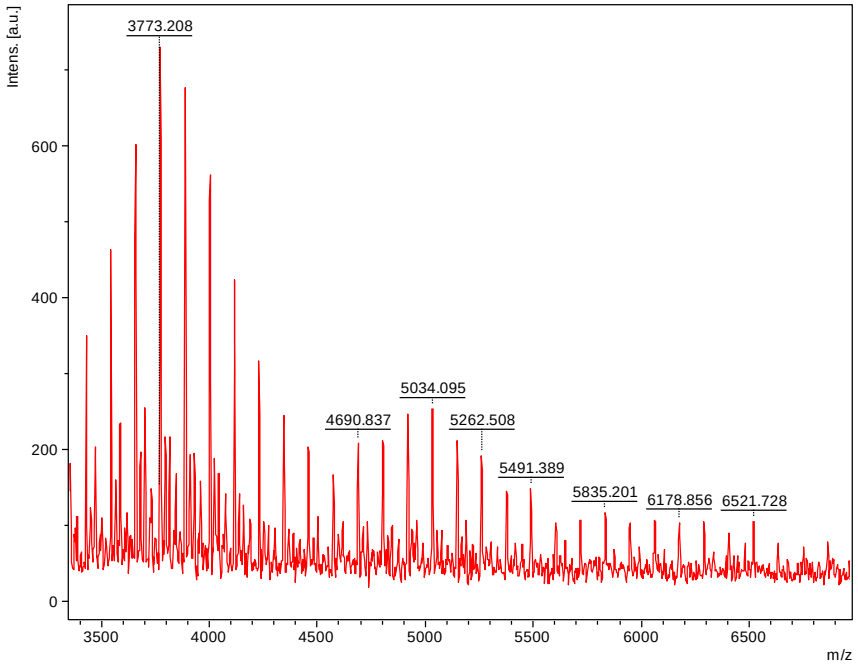

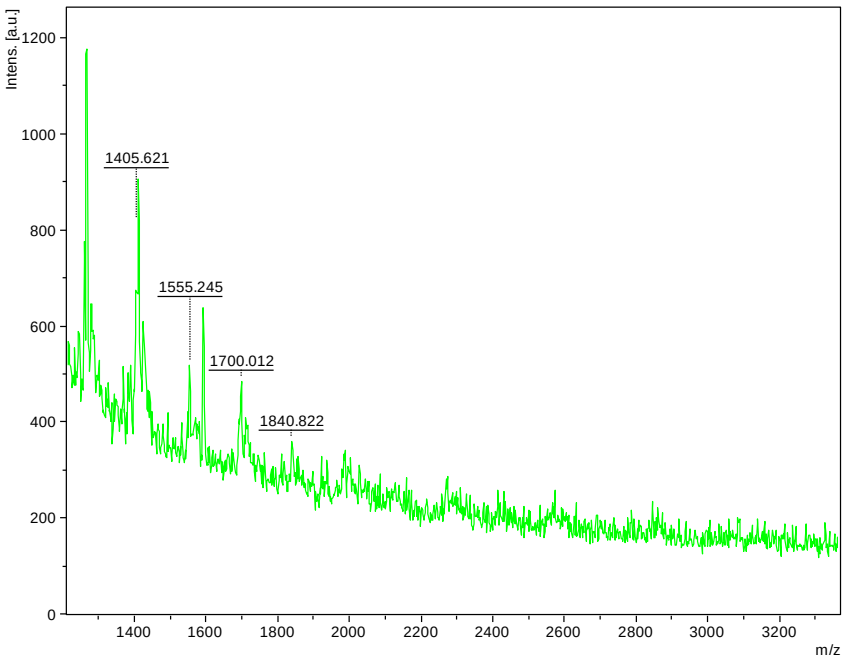

Figure S43. MALDI-ToF mass spectrum for Poly (ε-CL+*r*-LA), [Red: positive method in which we can see the gap of 114 which corresponding to the molecular weight of the ε-CL, Green: negative method in which we can see the gap of 144 which corresponding to the molecular weight of *r*-LA.

References

[1] G. M. Sheldrick, *Acta Cryst.* **2015**, *A71*, 3-8.

[2] D. F. Evans, *J. Phys. E: Sci. Instrum*., **1974**, *7*, 247.

[3] W. Yang, K. Q. Zhao,T. J. Prior, D. L. Hughes, A. Arbaoui, M. R. J. Elsegood and C. Redshaw, *Dalton Trans*., **2016**, *45*, 11990-12005.

[4] A. A. Abou-Hussein and W. Linert, *Spectrochim Acta A*., **2015**, *141*, 223-232.

[5] H. Sun, S. Xu, Z. Li, J. Xu, J. Liu, X. Wang, H. Wang, H. Dong, Y. Liu, K. Guo., *Polym. Ch em.*, **2017**, *8(36),* 5570-5509.

[6] S. Kan, Y. Jin, X. He, J. Chen, H. Wu, P. Ouyang, K. Guo and Z. Li., *Polym. Chem.*, **2013**, *4(21)*, 5432-5439.

[7] T. Rosen, I. Goldberg, W. Navarra, V. Venditto and M. Kol, *Angew. Chem*., **2018**, *130*, 7309-7313.